Int. J. Heat Mass Transfer. Vol. 34, No. 3, pp. 767–784, 1991
Printed in Great Britain

0017–9310/91 $3.00 + 0.00

Non-isothermal vapour absorption into falling film

NEIMA BRAUNER
Department of Fluid Mechanics and Heat Transfer, Faculty of Engineering, Tel-Aviv University, Ramat Aviv 69978, Israel

(*Received* 16 *November* 1989 *and in final form* 4 *May* 1990)

Abstract—The study relates to vapour absorption into a falling film, where the concentration levels of absorbate and absorbent are comparable. The combined heat and mass transfer processes involved are analysed through an integral formulation of the continuity, diffusion and energy equations. Adiabatic and isothermal wall conditions are considered. The Nusselt and Sherwood numbers are expressed in terms of the non-dimensional parameters which characterize the system. It is shown that in the case of finite absorbate dilution, the lateral convective term at the free interface ought to be accounted for. The resulting transfer rates are shown to depend on both the absorbate concentration level and driving force and are significantly augmented compared to those obtained under the assumption of infinite absorbate dilution.

1. INTRODUCTION

FILM TYPE heat and mass exchangers demonstrate high transfer coefficients at relatively low process driving force and are utilized extensively in a variety of industrial equipment, such as wetted wall columns, packed columns, rectifiers, evaporators, condensers and heat exchangers.

Of particular interest here is the process of hygroscopic condensation of relatively low temperature (low pressure) pure vapours on a hot film of an hygroscopic (salt) solution, which occurs due to the reduced vapour pressure of the sufficiently concentrated salt solution [1–4]. The driving force for condensation is the difference between the partial pressure of water in the brine solution and the partial pressure of the condensing (water) vapour. The condensation in this case is governed also by mass transfer mechanisms, due to a non-isothermal absorption, with a possible opposing thermal driving force in the condensing vapour phase. An important feature of the process is the comparable concentration levels of the absorbate (usually water) and the solute (salt), the former being usually the larger.

In utilizing a hygroscopic brine film as the condensing surface, the overall performance is governed by both the thermal resistance and the associated coupled resistance to mass transfer in the brine film, which is continuously varying due to the condensation at the free interface.

The process of hygroscopic condensation of water vapour on concentrated brine film has been described as a promising route for energy recovery from (naturally available) brines, which represents a storage of energy [4]. Clearly, the commercial applicability of the process to energy recovery schemes is highly dependent on the overall transfer rates that can be achieved.

Inspection of the relevant literature indicates that the focus has been mainly on the problem of absorption of sparingly soluble gases (infinite absorbate dilution) into a liquid film in isothermal conditions. These have been recently reviewed [5–8]. Relatively few studies accounted for the temperature variation. Yih and Seagrave [9] studied the effect of an a priori assumed temperature distribution across a laminar falling film on the physical properties, hence on the absorption process. Nakoryakov and Grigor'eva solved for the temperature profile [10, 11], assuming a uniform velocity across the film. The solutions for the coupled energy and diffusion equations were obtained in form of a series of eigenfunctions. Also presented in ref. [11], is an analytical solution for the temperature and concentration distribution at the entry region. Later on, Grossman [12, 13] improved the above model by eliminating the assumptions of uniform velocity across the film. Grossman and Heath [14], and Faghri and Seban [15, 16] extended the laminar model to turbulent flow conditions and widely discussed the heat and mass transfer coefficients for various operation conditions. These studies [9–17], which more specifically dealt with non-isothermal vapour absorption into hygroscopic solutions, while accounting for the coupling between energy and diffusion, still considered the process as of infinite absorbate dilution.

Recently Brauner *et al.* [18, 19] have shown that in film type absorption systems, where the absorbate concentration level is finite and comparable to that of the absorbent component (as in hygroscopic condensation), the convective term in the lateral direction is to be accounted for. The inclusion of the lateral convective term in the diffusion equations is of importance as it results in enhanced transfer rates. The applicability of results obtained, however, is limited to short transferring surfaces, due to the low penetration assumption involved in the analysis.

The present study is aimed at extending the analysis

NOMENCLATURE

c_p specific heat [kJ kg^{-1} K^{-1}]
C molar density [mol m^{-3}]
C_A absorbate concentration [mol m^{-3}]
C_B absorbent concentration [mol m^{-3}]
D diffusion coefficient [m^2 s^{-1}]
h film thickness [m]
h_T^* interfacial heat transfer coefficient [kJ m^{-2} s^{-1} K^{-1}]
h_{T_w} wall heat transfer coefficient [kJ m^{-2} s^{-1} K^{-1}]
H non-dimensional film thickness, h/h_i
Ja Jacob number, equation (18)
k thermal conductivity [kJ m^{-1} s^{-1} K^{-1}]
K mass transfer coefficient [m s^{-1}]
Le Lewis number, D/α
N molar flux [mol s^{-1} m^{-2}]
$\mathcal{N}$ non-dimensional molar flux, equation (19)
Nu Nusselt number, $h_T h_i/k$
Q_w non-dimensional heat flux, equation (42)
P vapour pressure [N m^{-2}]
Pe Peclet number, $\frac{3}{8}Re\,Pr$
Pr Prandtl number, $c_p\mu/k$
Re film Reynolds number, $4\Gamma/\mu$
Sc Schmidt number, ν/D
Sh Sherwood number, equation (77), Kh_i/D
Sh_n non-dimensional absorption flux, equation (76)
T temperature [K]
u downstream velocity [m s^{-1}]
U non-dimensional downstream velocity, equation (15)
v perpendicular velocity [m s^{-1}]
V non-dimensional downstream velocity, equation (15)
X_A molar fraction of absorbate
y perpendicular direction [m]
Y non-dimensional perpendicular direction, y/h
z downstream direction [m]
Z non-dimensional direction, z/h.

Greek symbols
α thermal diffusivity [m^2 s^{-1}]
α' surface inclination
β,γ constants, equation (20)
Γ liquid flow rate [kg s^{-1} m^{-1}]
δ boundary layer thickness [m]
Δ_θ non-dimensional thermal boundary layer thickness, δ_θ/h_i
Δ_ϕ non-dimensional concentration boundary layer thickness, δ_ϕ/h_i
η non-dimensional perpendicular coordinate, Y/H
θ non-dimensional temperature, equation (15)
λ^* molar heat of absorption [kJ kmol^{-1}]
Λ non-dimensional heat of absorption, equation (22)
μ viscosity [kg m^{-1} s^{-1}]
ν kinematic viscosity [m^2 s^{-1}]
ξ non-dimensional downstream coordinate, Z/Pe
ξ_θ value of ξ where firstly $\Delta_\theta = 1$
ξ_ϕ value of ξ where firstly $\Delta_\phi = 1$
ρ density [kg m^{-3}]
ϕ non-dimensional absorbate concentration, equation (15)
χ vapour quality
Ω enhancement factor, equation (70), $\mathcal{N}/\mathcal{N}^0$.

Subscripts
A absorbate
B non-volatile absorbent
c condensing vapour
i at inlet
n nominal
w at the wall
θ thermal
ϕ concentration.

Superscripts
* at equilibrium
¯ average
0 infinite dilution.

in order to elucidate and evaluate the effect of absorbate concentration level and process driving force downstream long transferring surfaces.

2. THE PHYSICAL MODEL AND GOVERNING EQUATIONS

The physical system and coordinates are schematically described in Fig. 1. A concentrated brine of a salt concentration C_{Bi}, water concentration C_{Ai} and temperature T_i, enters the condensation compartment at $z = 0$. It flows down over an inclined surface, in contact with pure stagnant saturated vapour (steam) at constant pressure P_c. The saturation temperature of the condensing vapour $T_c(P_c)$ may be lower than the brine temperature T_i. However, the relatively cold vapour may condense and be absorbed by the hotter brine film, provided the brine vapour pressure $P_A^*(T, C_A)$ is lower than P_c. In the absence of noncondensables, the resistance to absorption in the vapour phase is negligible and a liquid-phase controlled condensation–absorption is to be

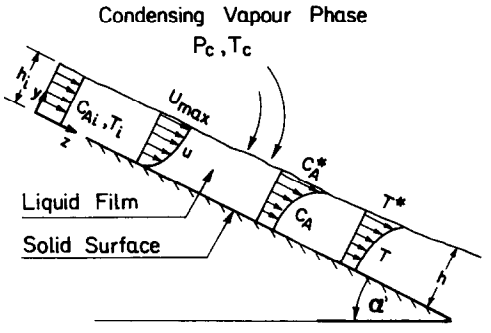

FIG. 1. Schematic description of the physical model and coordinates.

considered. Also, heat losses from the liquid phase to the adjacent condensing vapour are ignored. The heat released due to the hygroscopic condensation affects an increase of the brine temperature. Thus coupling between the mass and heat transfer processes results.

In formulating the governing equations it is assumed that the vapour absorption rate is small compared to the mass flow rate of the brine film. Therefore, the physical properties of the liquid film are considered to be constant.

The simultaneous mass and heat transfer in the system at steady state is described by the continuity, diffusion and energy equations:

$$\frac{\partial u}{\partial z}+\frac{\partial v}{\partial y}=0 \tag{1}$$

$$u\frac{\partial C_A}{\partial z}+v\frac{\partial C_A}{\partial y}=D\frac{\partial^2 C_A}{\partial y^2} \tag{2}$$

$$u\frac{\partial T}{\partial z}+v\frac{\partial T}{\partial y}=\alpha\frac{\partial^2 T}{\partial y^2} \tag{3}$$

where diffusion and heat conduction in the z-direction have been neglected with respect to those in the y-direction. The following boundary conditions apply:

$$z=0,\quad C_A=C_{Ai},\quad T=T_i$$

$$y=h,\quad C_A=C_A^*,\quad T=T^*(P_c,C_A^*)$$

$$y=0,\quad \frac{\partial C_A}{\partial y}=0$$

or

$$\begin{cases} T=T_w=T_i & \text{isothermal wall} \\ \dfrac{\partial T}{\partial y}=0 & \text{adiabatic wall} \end{cases} \tag{4}$$

where h is the local film thickness and C_A^* the absorbate interfacial concentration, assuming a vapour pressure equilibrium at the liquid free interface at temperature level T^* and external pressure level of the vapour phase, P_c. Note that though C_A^*, T^* are both unknown functions of z, they are related to each other by both the temperature–concentration–pressure equilibrium

$$P(C_A^*, T^*)=P_c=\text{const.} \tag{5}$$

and the condensation heat flux through the free interface

$$k\left.\frac{\partial T}{\partial y}\right|_{y=h}=\lambda_c^* N_{Ay}|_{y=h}. \tag{6}$$

Here $N_{Ay}|_{y=h}$ is the interfacial molar condensation flux, λ_c^* the molar heat of absorption of the condensing vapour which is a function of the interfacial conditions, C_A^*, T^*, and k the brine thermal conductivity. Clearly, equations (5) and (6) represent the coupling between the heat and mass transfer mechanisms.

The molar flux in the perpendicular direction, y, is given by

$$N_{Ay}=DC\frac{\partial X_A}{\partial y}+X_A(N_{Ay}+N_{By}). \tag{7}$$

The convective term in equation (7) can be omitted for either $X_A\to 0$ or $N_{Ay}=-N_{By}$, neither of which holds in the case of hygroscopic condensation. For instance, the minimum molar fraction of water, which corresponds to a saturated salt solution of $MgCl_2$, $CaCl_2$, LiBr, NaOH, is about $X_A\simeq 0.8$. However, since the salt is not transferred through the film free interface $N_{By}|_{y=h}\simeq 0$ may reasonably be assumed and equation (7) yields

$$N_{Ay}|_{y=h}=\left[\frac{D}{(1-X_A)}\frac{\partial C_A}{\partial y}\right]_{y=h}. \tag{8}$$

The velocity field (u, v) is to be obtained solving the momentum equations with the appropriate boundary condition: no-slip condition on the solid surface and no shear stress on the vapour–liquid interface. Assuming a fully developed flow prevails from the leading edge, and consistent with the assumption of low absorption rate (compared to the mass flow rate of the liquid film), the inertia terms in the momentum equations are neglected. In this case the downstream velocity $u(y)$ is given by the well-known Nusselt solution

$$u(y)=3\bar{u}\left[\frac{y}{h}-\frac{1}{2}\left(\frac{y}{h}\right)^2\right];\quad \bar{u}=\frac{\rho g\sin\alpha'}{3\mu}h^2 \tag{9}$$

where h, $\bar{u}$ are the local film thickness and corresponding average downstream velocity (both varying with z). Utilizing the velocity profile in an integral continuity condition yields the relationship between the local film thickness, the corresponding local mass flow rate, Γ, and the absorption–condensation molar flux at the free interface, whereby

$$N_{Ay}|_{y=h}=\frac{C}{\rho}\frac{d\Gamma}{dz}=C\frac{d}{dz}\int_0^h u\,dy=\frac{C\rho g\sin\alpha'}{\mu}h^2\frac{dh}{dz}. \tag{10}$$

The above formulation is rewritten in its dimensionless form. The non-dimensional presentations of

equations (1)–(3) and boundary conditions, equation (4), are

$$\frac{\partial U}{\partial Z}+\frac{\partial V}{\partial Y}=0 \tag{11}$$

$$U\frac{\partial \phi}{\partial Z}+V\frac{\partial \phi}{\partial Y}=\frac{Le}{Pe}\frac{\partial^2\phi}{\partial Y^2} \tag{12}$$

$$U\frac{\partial \theta}{\partial Z}+V\frac{\partial \theta}{\partial Y}=\frac{1}{Pe}\frac{\partial^2\theta}{\partial Y^2} \tag{13}$$

$$Z=0;\quad \phi=0;\quad \theta=0 \tag{14a}$$

$$Y=H;\quad \phi=\phi^*;\quad \theta=\theta^* \tag{14b}$$

$$Y=0;\quad \frac{\partial \phi}{\partial Y}=0 \tag{14c}$$

or

$$\begin{cases}\theta=0 & \text{isothermal wall}\\ \dfrac{\partial\theta}{\partial Y}=0 & \text{adiabatic wall}\end{cases}$$

where

$$Y=\frac{y}{h_i};\quad Z=\frac{z}{h_i};\qquad H=\frac{h}{h_i}$$

$$U=\frac{u}{\bar{u}_i}=3H^2\left[\frac{Y}{H}-\frac{1}{2}\left(\frac{Y}{H}\right)^2\right];\quad V=\frac{v}{\bar{u}_i}$$

$$\phi=\frac{C_A-C_{Ai}}{C^*_{Ai}-C_{Ai}};\quad \theta=\frac{T-T_i}{T_i^*-T_i}$$

$$Pe=\tfrac{1}{4}Re\,Pr;\quad Re=\frac{4\Gamma}{\mu}=\frac{4\bar{u}_i h_i}{\nu};$$

$$Pr=\nu/\alpha;\quad Le=\frac{D}{\alpha}=\frac{Pr}{Sc}. \tag{15}$$

Here, h_i, $\bar{u}_i$ denote the film thickness and corresponding average downstream velocity at $z=0$. C^*_{Ai} is the equilibrium concentration at the entry temperature T_i and vapour pressure P_c, $C^*_{Ai}=C^*_A(T_i,P_c)$ (and thus represents the interfacial concentration in the case of isothermal absorption). The equilibrium temperature $T_i^*=T^*(C_{Ai},P_c)$ includes the boiling point elevation corresponding to brine concentration C_{Ai} which is in equilibrium with its vapour at pressure P_c. In fact $T_i^*-T_i$ is a useful measure of the nominal available temperature driving force for the hygroscopic condensation process. Note that, the actual temperature drop T_c-T_i may be negative in the case of hygroscopic condensation, while condensation still takes place.

The dimensionless (unknown) interfacial temperature and concentration, ϕ^* and θ^*, are related to each other by the dimensionless form of equations (5) and (6)

$$P_c(\phi^*,\theta^*)=\text{const.} \tag{16}$$

$$\left.\frac{\partial\theta}{\partial Y}\right|_{Y=H}=\frac{Pe}{Ja}\mathcal{N}. \tag{17}$$

Here Ja denotes the Jacob number

$$Ja=\frac{\rho c_p(T_i^*-T_i)}{C\lambda_c^*} \tag{18}$$

and $\mathcal{N}$ the dimensionless molar flux of condensation at the free interface, which by equations (8) and (15) reads

$$\mathcal{N}=\frac{1}{C\bar{u}_i}N_{Ai}|_{Y=H}=-\frac{Le}{Pe}\frac{\gamma}{(\gamma\phi^*+\beta)}\left.\frac{\partial\phi}{\partial Y}\right|_{Y=H} \tag{19}$$

$$\gamma=(C_{Ai}-C^*_{Ai})/C;\quad \beta=1-C_{Ai}/C. \tag{20}$$

Note that γ represents a nominal driving force process. Combining equations (17) and (19) yields a relation between temperature and concentration gradients to be satisfied at the film free interface

$$\left.\frac{\partial\theta}{\partial Y}\right|_{Y=H}=-\frac{\gamma\,Le}{Ja}\frac{1}{\gamma\phi^*+\beta}\left.\frac{\partial\phi}{\partial Y}\right|_{Y=H}=\frac{\Lambda}{\gamma\phi^*+\beta}\left.\frac{\partial\phi}{\partial Y}\right|_{Y=H} \tag{21}$$

where Λ is a dimensionless heat of condensation–absorption defined by

$$\Lambda=\frac{Le\,\lambda_c^*(C^*_{Ai}-C_{Ai})}{\rho c_p(T_i^*-T_i)}=\frac{-\gamma\,Le}{Ja}. \tag{22}$$

Clearly, in order to proceed with the solution it is required to specify an equilibrium relation between temperature, composition and vapour pressure (equation (16)). Experimental data, available in the literature for various brines is usually formulated in a linear relation between temperature, composition and the logarithm of the vapour pressure at equilibrium [12]. Under conditions of constant vapour pressure, P_c, a linear relation specifies, $C_A^*=a_1T^*+a_2$, which in terms of the dimensionless concentration and temperature defined in equation (15), reads

$$\phi^*+\theta^*=1. \tag{23}$$

The solution also requires data of the latent heat condensation of vapour over the brine interface $\lambda_c^*(C_A^*,T^*)$, which is given by [4]

$$\lambda_c^*=\lambda^*|_{C_A^*,T^*}-c_{pc}(T^*-T_c)-(1-\chi)\lambda \tag{24}$$

where λ^* is the heat of evaporation (or condensation) of a unit mass of pure water from a solution of concentration C_A^*, which is in thermodynamic equilibrium with its (superheated) vapour at a temperature T^*. Equation (24) includes a correction of λ^* for the sensible heat losses due to condensation of relative cold vapour at temperature $T_c\leqslant T^*$ with a specific heat c_{pc}, and for the latent heat loss when vapour condensation of quality $\chi<1$ is involved. For absorption of water vapour the dependence of λ_c^* on C_A^* and T^* is known to be rather weak, and a constant λ_c^* (constant Λ and Ja) is assumed.

3. SOLUTION OF THE GOVERNING EQUATIONS—INTEGRAL FORMULATION

In the case of absorption of sparingly soluble gases, $X_A \ll 1$, convection in the perpendicular direction is negligible and the term of $(1-X_A)$ in equation (8) degenerates to 1, or $\gamma\phi+\beta \to 1$ in equations (19) and (21). When a constant film thickness is also assumed, the formulation reduces to the coupled heat and mass diffusion equations solved by Grossman [12].

For the finite concentration level of the absorbed component as in hygroscopic condensation, equations (17)–(19) yield a non-linear relation (in terms of the unknown function ϕ), which makes the exact approach to the solutions of the partial differential equations unamenable. Recently, an exact solution for finite absorbate concentration was presented [18, 19], assuming low penetration of the (heat and mass) boundary layers. However, the validity of this solution is restricted to a short transferring surface. Here, in order to extend the analysis of the effect of finite absorbate concentration level on the associated mass and heat transfer rates downstream, an integral approach is employed.

The integral formulation is obtained by integrating equations (11)–(13) across the local film thickness H, while utilizing equations (14), (17)–(19). The corresponding integral continuity, diffusion and energy equations read

$$\mathcal{N} = \frac{1}{Pe}\frac{\mathrm{d}}{\mathrm{d}\xi}\int_0^1 HU\,\mathrm{d}\eta = -V|_{\eta=1}; \quad \text{continuity} \tag{25}$$

$$\frac{\mathrm{d}}{\mathrm{d}\xi}\int_0^1 HU\phi\,\mathrm{d}\eta = \frac{Le\,\beta}{H}\frac{1}{\gamma\phi^*+\beta}\left.\frac{\partial\phi}{\partial\eta}\right|_{\eta=1}; \quad \text{diffusion} \tag{26}$$

$$\frac{\mathrm{d}}{\mathrm{d}\xi}\int_0^1 HU\theta\,\mathrm{d}\eta - \frac{1}{Ja}(Ja\,\theta^*+1)\frac{\mathrm{d}}{\mathrm{d}\xi}\int_0^1 HU\,\mathrm{d}\eta = -\frac{1}{H}\left.\frac{\partial\theta}{\partial\eta}\right|_{\eta=0}; \quad \text{energy} \tag{27}$$

where

$$\eta = \frac{y}{h} = \frac{Y}{H}; \quad \xi = Z/Pe. \tag{28}$$

The solution of the diffusion and energy requires that the concentration and temperature profiles across the film will be specified (the velocity profile is given in equation (15)). The assumed profiles are chosen so as to match the boundary conditions and the physical situation prevailing downstream. As the liquid entering at $z = 0$ is at a state of nonequilibrium with the vapour phase, a process of simultaneous heat and mass transfer sets in at the free interface and extends its effect gradually into the film. Hence, the mass and thermal boundary layers grow in the downstream direction until they occupy the entire depth of the film. The shapes of the concentration and temperature profiles are formulated in accordance with the relative thickness of the corresponding boundary layers.

3.1. *Concentration profiles*

Denoting the downstream location where the concentration boundary layer, δ_ϕ, first occupies the entire depth of the film by ξ_ϕ, the developing boundary layer region, where $\Delta_\phi = \delta_\phi/h \leqslant 1$, extends over $0 \leqslant \xi \leqslant \xi_\phi$. In this region, a concentration profile, shaped in terms of the local boundary layer thickness, $\Delta_\phi(\xi)$, which satisfies boundary conditions (14b) and (14c) reads

$$\phi = \begin{cases} 0; & \text{for } 0 \leqslant \eta \leqslant (1-\Delta_\phi) \\ \phi^*[(1-\Delta_\phi-\eta)/\Delta_\phi]^2; & \text{for } (1-\Delta_\phi) < \eta \leqslant 1 \end{cases} \qquad 0 \leqslant \xi \leqslant \xi_\phi \tag{29}$$

whereby

$$\left.\frac{\partial\phi}{\partial\eta}\right|_{\eta=1} = \frac{2\phi^*}{\Delta_\phi}. \tag{30}$$

Note that equation (29) also satisfies $\phi = 0$ and $\partial\phi/\partial\eta = 0$ at the edge of the diffusion boundary layer, $\eta = 1-\Delta_\phi$. The corresponding bulk concentration in this developing region reads

$$\bar{\phi} = \int_0^1 U\phi\,\mathrm{d}\eta = \frac{H^2\phi^*}{2}\left[\Delta_\phi - \frac{\Delta_\phi^3}{10}\right]; \quad 0 \leqslant \xi \leqslant \xi_\phi. \tag{31}$$

In the fully developed boundary layer region, where $\xi > \xi_\phi$ and $\Delta_\phi \equiv 1$, the concentration profile is shaped in terms of the (unknown) dimensionless concentration at the wall, $\phi_w(\xi)$, to match boundary conditions (14b) and (14c)

$$\phi = \phi_w + (\phi^* - \phi_w)\eta^2; \quad \xi \geqslant \xi_\phi \tag{32}$$

whereby

$$\left.\frac{\partial\phi}{\partial\eta}\right|_{\eta=1} = 2(\phi^* - \phi_w) \tag{33}$$

and

$$\phi_w = 0 \quad \text{at} \quad \xi = \xi_\phi. \tag{34}$$

The bulk concentration in the developed layer region reads

$$\bar{\phi} = \int_0^1 U\phi\,\mathrm{d}\eta = \frac{H^2}{20}(9\phi^* + 11\phi_w); \quad \xi > \xi_\phi. \tag{35}$$

Note that at $\xi = \xi_\phi$, where $\Delta_\phi = 1$ and $\phi_w = 0$, equations (29), (32) and (31), (35) yield identical expressions ($\phi = \phi^*\eta^2$ and $\bar{\phi} = 9H^2\phi^*/20$).

3.2. *Temperature profiles*

The developing boundary layer region, $\Delta_\theta = \delta_\theta/h \leqslant 1$, extends over $0 \leqslant \xi \leqslant \xi_\theta$, with ξ_θ denoting the downstream distance where the thermal boundary

layer thickness reaches the (local) film thickness. The temperature profile in this region is shaped in terms of the local thermal boundary layer thickness, Δ_θ, to match boundary conditions (14b) and (14c)

$$\theta = \begin{cases} 0; & \text{for } 0 \leqslant \eta \leqslant 1-\Delta_\theta \\ \theta^*[(1-\Delta_\theta-\eta)/\Delta_\theta]^2; & \text{for } 1-\Delta_\theta < \eta \leqslant 1 \end{cases}$$

$$0 \leqslant \xi \leqslant \xi_\theta \quad (36)$$

whereby

$$\left.\frac{\partial\theta}{\partial\eta}\right|_{\eta=1} = \frac{2\theta^*}{\Delta_\theta}. \quad (37)$$

The corresponding bulk temperature reads

$$\bar{\theta} = \int_0^1 U\theta \, d\eta = \frac{H^2\theta^*}{2}\left(\Delta_\theta - \frac{\Delta_\theta^3}{10}\right) \quad 0 \leqslant \xi \leqslant \xi_\theta. \quad (38)$$

Note that equation (36) also satisfies $\theta = 0$ and $\partial\theta/\partial\eta = 0$ at $\eta = 1-\Delta_\theta$. Equations (36)–(38) apply to both the constant temperature wall and the adiabatic wall cases.

In the region where the thermal boundary layer becomes fully developed, $\Delta_\theta \equiv 1$ and $\xi > \xi_\theta$, a distinction is to be made between the profile assumed for the isothermal and adiabatic wall cases. For an isothermal wall, equation (14c) requires $\theta_w = 0$, and the temperature profile is shaped in terms of the (unknown) dimensionless heat flux at the wall, $Q_w(\xi)$. The assumed profile, which satisfies boundary conditions (14b) and (14c), and the corresponding bulk temperature are given by

$$\theta = Q_w\eta + (\theta^* - Q_w)\eta^2 \quad \xi \geqslant \xi_\theta, \quad \theta_w \equiv 0 \quad (39)$$

$$\bar{\theta} = \int_0^1 U\theta \, d\eta = \frac{H^2}{40}[18\theta^* + 7Q_w]$$

$$\xi \geqslant \xi_\theta, \quad \theta_w \equiv 0 \quad (40)$$

whereby

$$\left.\frac{\partial\theta}{\partial\eta}\right|_{\eta=1} = 2\theta^* - Q_w \quad (41)$$

$$Q_w \equiv \left.\frac{\partial\theta}{\partial\eta}\right|_{\eta=0} \quad (42)$$

and

$$Q_w \equiv 0 \quad \text{at} \quad \xi = \xi_\theta.$$

For the adiabatic wall case, $Q_w \equiv 0$ by equation (14c), and the assumed temperature profile, shaped in terms of the unknown wall temperature, $\theta_w(\xi)$, which satisfies boundary conditions (14b) and (14c) reads

$$\theta = \theta_w + (\theta^* - \theta_w)\eta^2 \quad \xi \geqslant \xi_\theta; \quad Q_w \equiv 0 \quad (43)$$

$$\bar{\theta} = \frac{H^2}{20}(9\theta^* + 11\theta_w) \quad \xi \geqslant \xi_\theta; \quad Q_w \equiv 0 \quad (44)$$

whereby

$$\left.\frac{\partial\theta}{\partial\eta}\right|_{\eta=1} = 2(\theta^* - \theta_w) \quad (45)$$

and

$$\theta_w = 0 \quad \text{at} \quad \xi = \xi_\theta.$$

The assumed profiles ensure a smooth transition at $\xi = \xi_\theta$, $\Delta_\theta \equiv 1$, since equations (36), (39) and (43) all yield $\theta = \theta^*\eta^2$ at $\xi = \xi_\theta$ and the corresponding $\bar{\theta}$, by equations (38), (40) and (44), reads $\bar{\theta} = 9H^2\theta^*/20$.

Substituting the above velocity, concentration and temperature profiles in equations (25)–(27) and carrying out the integration over the film thickness yields:

Continuity equation

$$\mathcal{N} = \frac{3}{Pe}H^2\frac{dH}{d\xi}. \quad (46)$$

Diffusion equation

$$\frac{d}{d\xi}\left[\frac{H^3\phi^*}{2}\left(\Delta_\phi - \frac{\Delta_\phi^3}{10}\right)\right]$$

$$= -\frac{\beta Pe}{\gamma}\mathcal{N} = \frac{2Le\,\beta}{H}\frac{\phi^*}{\Delta_\phi(\gamma\phi^* + \beta)}$$

$$\mathcal{N} = \frac{-2\gamma Le}{H Pe}\frac{\phi^*}{\Delta_\phi(\gamma\phi^* + \beta)}; \quad 0 \leqslant \xi \leqslant \xi_\phi \quad (47a)$$

$$\frac{d}{d\xi}\left[\frac{H^3}{20}(9\phi^* + 11\phi_w)\right] = \frac{2Le\,\beta}{(\gamma\phi^* + \beta)}(\phi^* - \phi_w)$$

$$\mathcal{N} = \frac{-2\gamma Le}{H}\frac{(\phi^* - \phi_w)}{(\gamma\phi^* + \beta)}; \quad \xi \geqslant \xi_\phi. \quad (47b)$$

Energy equation

$$\frac{d}{d\xi}\left[\frac{H^3\theta^*}{2}\left(\Delta_\theta - \frac{\Delta_\theta^3}{10}\right)\right] = \frac{Pe}{Ja}(Ja\,\theta^* + 1)\mathcal{N}$$

$$\left.\frac{\partial\theta}{\partial\eta}\right|_{\eta=1} = \frac{2\theta^*}{\Delta_\theta}; \quad 0 \leqslant \xi \leqslant \xi_\theta. \quad (48a)$$

For isothermal wall and $\xi \geqslant \xi_\theta$

$$\frac{d}{d\xi}\left[\frac{H^3}{40}(18\theta^* + 7Q_w)\right] = \frac{Pe}{Ja}(Ja\,\theta^* + 1)\mathcal{N} - \frac{Q_w}{H}$$

$$\left.\frac{\partial\theta}{\partial\eta}\right|_{\eta=1} = 2\theta^* - Q_w; \quad \theta_w \equiv 0; \quad \xi \geqslant \xi_\theta \quad (48b)$$

or for adiabatic wall and $\xi \geqslant \xi_\theta$

$$\frac{d}{d\xi}\left[\frac{H^3}{20}(9\theta^* + 11\theta_w)\right] = \frac{Pe}{Ja}(Ja\,\theta^* + 1)N$$

$$\left.\frac{\partial\theta}{\partial\eta}\right|_{\eta=1} = 2(\theta^* - \theta_w); \quad Q_w \equiv 0; \quad \xi \geqslant \xi_\theta. \quad (48c)$$

Equations (46)–(48) with equation (17) and the equilibrium condition at the free interface, equation (23), provide five equations to be solved for the following five unknowns: H, θ^*, ϕ^*, $\Delta_\phi(\xi \leqslant \xi_\phi)$ or $\phi_w(\xi > \xi_\phi)$, and $\Delta_\theta(\xi < \xi_\theta)$ alternating with $Q_w(\xi > \xi_\theta)$ for iso-

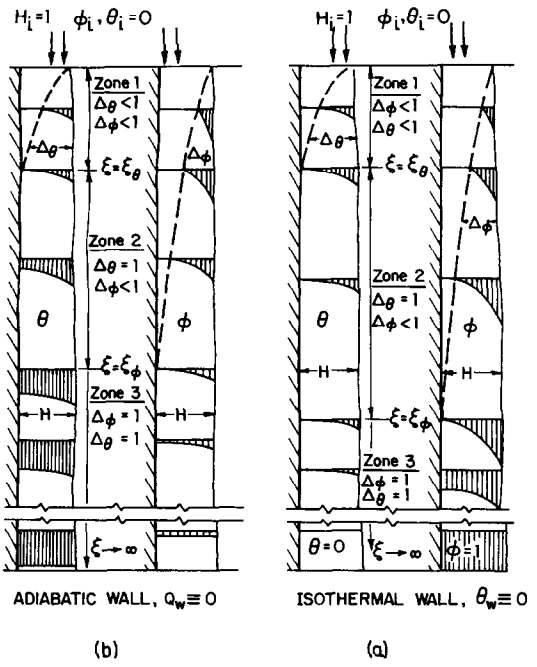

FIG. 2. Schematic description of the various integration zones.

thermal wall or with $\theta_w(\xi > \xi_\theta)$ for adiabatic wall conditions. All are functions of the downstream distance, ξ.

The boundary conditions used for solving the three simultaneous first-order differential equations, equations (46)–(48), are

$$\Delta_\phi = 0; \quad \Delta_\theta = 0; \quad H = 1 \quad \text{at} \quad \xi = 0. \tag{49}$$

It is to be noted that, consistent with the concentration and velocity profiles used in the derivation, $\phi_w \equiv 0$ for $\xi \leqslant \xi_\phi$ and Q_w, $\theta_w \equiv 0$ for $\xi \leqslant \xi_\theta$. Thus, the values of the relevant variables at the transition points from the developing boundary layer regions to the fully developed boundary layer regions (at $\xi = \xi_\phi$ where $\Delta_\phi = 1$ or at $\xi = \xi_\theta$ where $\Delta_\theta = 1$), are defined as well.

Figure 2 schematically identifies the three integration zones. In zone 1 both the thermal and concentration boundary layers are developing; in zone 2 one is fully developed and the other still developing; and in zone 3 both boundary layers are fully developed. The exact forms of the differential equations, used for integration in each zone, are detailed in Appendix A.

A computer program was set for integrating the above system, starting with the initial values defined in equation (49), using a Runge–Kutta type method. The procedure performs an integration step and the results of each step serves as input for the next one. The step size is automatically controlled according to the accuracy requirements and speed considerations.

Calculated results and discussion are presented below (Section 6). Analytic solutions obtained under the assumption of low penetration and for isothermal absorption follows.

4. LOW PENETRATION (ZONE 1)

The equations prevailing in the first zone are equations (46), (47a) and (48a). For relatively short exposure time ($\xi \ll \xi_\theta, \xi_\phi$) the thermal and diffusion boundary layers are limited to the near free interface region with $\Delta_\theta, \Delta_\phi \ll 1$.

Eliminating $\mathcal{N}$ between equations (47a) and (48a) for $Ja\,\theta^* \ll 1$, and integrating the resulting differential equation while applying boundary condition (49), yields

$$H^3\theta^*\Delta_\theta\left(1-\frac{\Delta_\theta^2}{10}\right) = -\frac{\gamma H^3}{\beta Ja}\phi^*\Delta_\phi\left(1-\frac{\Delta_\phi^2}{10}\right). \tag{50}$$

Combining boundary conditions (17) and (23) yields

$$\frac{\Delta_\phi}{\Delta_\theta} = \frac{\Lambda\phi^*}{(1-\phi^*)(\gamma\phi^*+\beta)}; \quad \Lambda = -\frac{\gamma\, Le}{Ja}. \tag{51}$$

For $\Delta_\theta, \Delta_\phi \ll 1$, equation (50) reads

$$-\frac{\gamma}{\beta Ja}\frac{\phi^*}{\theta^*}\frac{\Delta_\phi}{\Delta_\theta} = 1. \tag{52}$$

Eliminating $\Delta_\phi/\Delta_\theta$ between equations (51) and (52) results in the following cubic equation for ϕ^*

$$\frac{1}{(\gamma\phi^*+\beta)}\left[\frac{\phi^*}{1-\phi^*}\right]^2 = \frac{\beta\, Le}{\Lambda^2} \tag{53a}$$

or

$$\gamma\phi^{*3}+\left(\beta-2\gamma-\frac{\Lambda^2}{\beta\, Le}\right)\phi^{*2}+(\gamma-2\beta)\phi^*+\beta = 0. \tag{53b}$$

Thus, in the entry region and for sufficiently small ξ, where the low penetration assumption is valid, ϕ^*, θ^* are constant (ξ independent) and determined by the parameters β, γ, Λ and Le. Substituting the solution obtained for ϕ^* in equation (51) yields the corresponding $\Delta_\phi/\Delta_\theta$ in this region. Note that equation (53a) may be used to derive $\phi^*(\xi = 0)$, a boundary condition which is applied in the integration procedure (see Appendix A).

For finite dilution, $\beta < 1$, but in the limit of low driving force, $\gamma \to 0$, equation (53b) yields

$$\phi^* = \frac{1}{1+\Lambda/(\beta\sqrt{(Le)})};$$

$$\theta^* = 1-\phi^* = \frac{\Lambda/(\beta\sqrt{(Le)})}{1+\Lambda/(\beta\sqrt{(Le)})} \tag{54a}$$

while for infinite dilution of absorbate, as in the case of sparingly soluble gases, both $\gamma\phi^* \to 0$ and $\beta \to 1$, and the solution of equation (53b) reads

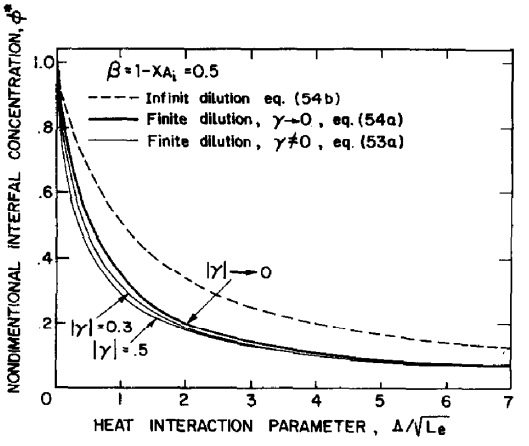

FIG. 3. Interfacial absorbate concentration in the low penetration region.

$$\phi^{*0} = \frac{1}{\Lambda/\sqrt{(Le)}+1};$$

$$\theta^{*0} = 1-\phi^{*0} = \frac{\Lambda/\sqrt{(Le)}}{\Lambda/\sqrt{(Le)}+1}. \qquad (54b)$$

Equation (54b) is identical with the exact analytical solution given by Grigor'eva and Nakoryakov [10].

The effect of finite absorbate concentration level is demonstrated in Fig. 3, for $\beta = 1-X_{Ai} = 0.5$ and various heat interaction parameters $\Lambda/\sqrt{(Le)}$. It is shown that with increasing the absorbate concentration levels the interfacial equilibrium concentration significantly deviates from the values obtained under the assumption of infinite absorbate dilution. The decrease of interfacial concentration, ϕ^*, with increasing the absorbate concentration and the nominal driving force $|\gamma|$ evolves from heating-up of the film interface by the enhanced absorption rates, as will be further discussed below. These trends are consistent with the exact solution recently obtained for the low penetration region [19].

The variation of H, Δ_ϕ and Δ_θ in the downstream direction is derived by substituting equation (51), in the continuity, diffusion and thermal equations (46), (47a) and (48a), which for $\Delta_\phi, \Delta_\theta \ll 1$, read

$$\frac{dH}{d\xi} = -\frac{2\gamma\, Le}{3H^3}\frac{\phi^*}{(\gamma\phi^*+\beta)\Delta_\phi}; \quad H(\xi=0)=1 \qquad (55)$$

$$\frac{d\Delta_\phi}{d\xi} = \frac{4Le\beta}{H^4}\frac{1}{(\gamma\phi^*+\beta)\Delta_\phi}; \quad \Delta_\phi(\xi=0)=0 \qquad (56)$$

$$\frac{d\Delta_\theta}{d\xi} = \frac{4}{H^4\Delta_\theta}; \quad \Delta_\theta(\xi=0)=0. \qquad (57)$$

By equations (55) and (56)

$$\frac{dH}{d\Delta_\phi} = -\frac{1}{6}\frac{\gamma}{\beta}H; \quad H(\Delta_\phi=0)=1. \qquad (58)$$

Integrating equation (58) yields $H(\Delta_\phi)$, whereby

$$H = e^{-(\gamma/6\beta)\Delta_\phi} \qquad (59)$$

while substitution of equation (59) in equation (56) and integration yields an equation for $\Delta_\phi(\xi)$

$$1-\exp\left[-\frac{2}{3}\frac{\gamma}{\beta}\Delta_\phi\left(\frac{2}{3}\frac{\gamma}{\beta}\Delta_\phi+1\right)\right] = \frac{16}{9}\frac{Le\gamma^2}{\beta}\frac{\xi}{(\gamma\phi^*+\beta)}. \qquad (60)$$

As indicated by equation (59), for a sufficiently low process driving force $|\gamma| = (C^*_{Ai}-C_{Ai})/C < 1$, $|\gamma|\Delta_\phi \ll 1$ and thus $H = 1$ may reasonably be assumed. In this case the integration of equations (56) and (57) yields

$$\Delta_\phi = \left[\frac{8Le\beta}{(\gamma\phi^*+\beta)}\xi\right]^{1/2} = \left[\frac{8Le(1-X_{Ai})}{(1-X^*_A)}\xi\right]^{1/2} \qquad (61)$$

$$\Delta_\theta = \sqrt{(8\xi)} \qquad (62)$$

or

$$\frac{\Delta_\phi}{\Delta_\theta} = \left[\frac{Le(1-X_{Ai})}{(1-X^*_A)}\right]^{1/2} \qquad (63)$$

and with X_{Ai}, $X^*_A \to 0$ (infinite absorbate dilution) $\Delta_\phi/\Delta_\theta = \sqrt{(Le)}$.

For most absorbent liquids $Le \ll 1$, and therefore the thermal boundary layer is expected to become fully developed when the concentration boundary layer is still quite thin. For finite dilution however, an enhanced growth of the diffusion boundary layer is predicted by equation (63), and $\Delta_\phi > \Delta_\theta$ may result even with $Le < 1$.

Note that equations (54) imply that for sufficiently low driving force, the solution for the temperature and concentration profiles for finite dilution are identical to those obtained for infinite dilution, when Λ is replaced by Λ/β. Inspection of the general formulation, in equations (46)–(48), reveals that this observation is not specific to the low penetration region but valid everywhere downstream (see Appendix B).

5. ISOTHERMAL ABSORPTION

In some cases the heat interaction is small and the process maybe considered isothermal, with both Λ and θ identically zero and $\phi^* \equiv 1$. The effect of finite absorbate concentration level is explored here for sufficiently low absorption driving force (small γ), where a constant film thickness, $H = 1$, may reasonably be assumed. In this case only the diffusion equation is to be considered.

5.1. *Zone 1*: $\Delta_\phi \leqslant 1$ *and* $\xi \leqslant \xi_\phi$

Equation (47a) reduces to

$$\frac{d}{d\xi}[\Delta_\phi - \Delta_\phi^3/10] = \frac{4Le\beta}{(\gamma+\beta)}\frac{1}{\Delta_\phi}; \quad \Delta_\phi(\xi=0)=0$$

$$\mathcal{N} = \frac{-2Le}{Pe}\frac{\gamma}{\gamma+\beta}\frac{1}{\Delta_\phi}. \tag{64}$$

Integration yields

$$\Delta_\phi^2\left(1-\frac{3}{20}\Delta_\phi^2\right) = \frac{8Le\beta}{(\gamma+\beta)}\xi. \tag{65}$$

Equation (65) is solved for $\Delta_\phi(\xi)$

$$\Delta_\phi = \left\{\frac{10}{3}\left[1-\left(1-\frac{24}{5}\frac{Le}{(\gamma/\beta+1)}\xi\right)^{1/2}\right]\right\}^{1/2} \tag{66}$$

or

$$\frac{\Delta_\phi}{\Delta_\phi^0} = \left\{\frac{\left[1-\left(1-\frac{24}{5}\frac{Le\,\xi}{\gamma/\beta+1}\right)^{1/2}\right]}{\left[1-\left(1-\frac{24}{5}Le\,\xi\right)^{1/2}\right]}\right\} \tag{67}$$

where Δ_ϕ^0 denotes the corresponding value obtained for infinite absorbate dilution ($\gamma \to 0$ and $\beta \to 1$). For $\Delta_\phi \ll 1$ (low penetration), equation (65) yields

$$\Delta_\phi = \left(\frac{1}{\gamma/\beta+1}\right)^{1/2}(8Le\,\xi)^{1/2}; \quad \frac{\Delta_\phi}{\Delta_\phi^0} = \left(\frac{1}{\gamma/\beta+1}\right)^{1/2}. \tag{68}$$

The corresponding solution for the average concentration is obtained by substituting Δ_ϕ by equation (66) in equation (31) (with $\phi^* = 1$ and $H = 1$). Note that since $\gamma < 0$ (see equation (20)) $\Delta_\phi/\Delta_\phi^0 > 1$, and an enhanced growth of the diffusion boundary layer with increasing the absorbate concentration level (decreasing β) is predicted. Solving equation (66) for $\Delta_\phi = 1$ yields the downstream location where the boundary layer becomes fully developed

$$\xi_\phi = \frac{17}{160}\frac{(\gamma/\beta+1)}{Le}; \quad \frac{\xi_\phi}{\xi_\phi^0} = (\gamma/\beta+1). \tag{69}$$

As expected, $\xi_\phi < \xi_\phi^0$ results.

The corresponding absorption flux at the film free interface is obtained by substituting the solution obtained $\Delta_\phi(\xi)$ in the expression for $\mathcal{N}$, given in equation (64). An enhancement factor, Ω, is introduced, which expresses the ratio between the actual absorption flux, $\mathcal{N}$, and that obtained under the assumption of infinite dilution, $\mathcal{N}^0$

$$\Omega = \frac{\mathcal{N}}{\mathcal{N}^0} = \frac{1}{\beta(1+\gamma/\beta)}\frac{\Delta_\phi^0}{\Delta_\phi}. \tag{70}$$

For instance, when equation (68) is substituted for $\Delta_\phi/\Delta_\phi^0$ (low penetration region)

$$\Omega = \frac{1}{\beta(\gamma/\beta+1)^{1/2}}. \tag{71}$$

As is indicated by equations (70) and (71) the effect of finite dilution, as represented by $\beta < 1$ and $\gamma < 0$, results in an enhanced absorption flux, with $\Omega \geqslant 1$. The predicted enhancement evolves from retaining the convective term in the interfacial absorption flux (equations (7) and (8)). The results of equation (71) are consistent with the finite dilution enhancement effect recently predicted in refs. [18, 19].

5.2. *Zone 2*: $\Delta_\phi \equiv 1$, $\xi > \xi_\phi$

Equation (47b) reduces to

$$\frac{\mathrm{d}}{\mathrm{d}\xi}\left[\frac{1}{20}(9+11\phi_w)\right] = \frac{2Le\,\beta}{\gamma+\beta}(1-\phi_w);$$

$$\phi_w(\xi = \xi_\phi) = 0$$

$$\mathcal{N} = \frac{-2Le\,\gamma}{Pe(\gamma+\beta)}(1-\phi_w). \tag{72}$$

Integration yields

$$\phi_w = 1-\exp\left[-\frac{40}{11}\frac{Le}{\gamma/\beta+1}(\xi-\xi_\phi)\right]. \tag{73}$$

The corresponding solution for the average concentration is obtained by substituting the solution for $\phi_w(\xi)$ in equations (32) and (35) (with $\phi^* = 1, H = 1$). Combining equations (69), (72) and (73) yields the amplification due to the convective term, which evolves for finite absorbate dilution with $\beta < 1$ and $\gamma < 0$

$$\Omega = \frac{\mathcal{N}}{\mathcal{N}^0} = \frac{1}{\beta(\gamma/\beta+1)}\exp\left[\frac{40}{11}\frac{\gamma/\beta\,Le\,\xi}{\gamma/\beta+1}\right];$$

$$Le\,\xi = \frac{Z}{Re\,Sc}. \tag{74}$$

Note that since $\gamma < 0$, an exponential decay of the enhancement is predicted in the downstream direction.

6. RESULTS AND DISCUSSION

As is indicated by equations (46)–(48), the solutions for the non-dimensional concentration of the absorbate and temperature profile are determined by the concentration level, $C_{Ai}/C = 1-\beta$, the nominal driving force $\gamma = (C_{Ai}^* - C_{Ai})/C$, heat of absorption Λ and the Le of the solutions involved. Note that Pe does not appear explicitly upon substitution of $\mathcal{N}$, and Ja is related to the other parameters as in equation (22). The calculated results are presented in what follows in terms of these non-dimensional parameters. The various cases considered are summarized in Table 1.

Figures 4 and 5 present typical variation of the concentrations and temperatures in the absorbing film with the non-dimensional downstream distance $\xi = z/(h_i\,Pe)$. Curves are given for the calculated interfacial and wall concentrations ϕ^*, ϕ_w (Fig. 4), temperatures θ^*, θ_w (Fig. 5) and the corresponding variation of the thermal and concentration boundary layers (Fig. 6) for isothermal wall and adiabatic wall conditions. The effect of the absorbate concentration level is studied by varying β and maintaining a low driving force ($\gamma \to 0$). Some relevant analytic

Table 1.

Case studied		Model equations	Related figures
General non-isothermal vapour absorption $\gamma, \beta, \Lambda \neq 0$	Isothermal wall	(46), (47), (48a) or (48b)	9, 10
	Adiabatic wall	(46), (47), (48a) or (48c)	
Non-isothermal low nominal driving force $\gamma \to 0; \beta, \Lambda \neq 0$	Isothermal wall	Appendix B	4(a), 5(a), 6(a), 7(a), (c), 8(a)
	Adiabatic wall		4(b), 5(b), 6(b), 7(b), 8(b)
Non-isothermal low penetration $\gamma, \beta, \Lambda \neq 0; \Delta_\theta, \Delta_\phi \ll 1$	Isothermal or adiabatic wall	Section 4	3
Isothermal absorption $\Lambda = 0; \gamma, \beta \neq 0$		Section 5	

expressions for this particular case are derived in Appendix B. For infinite absorbate dilution $\gamma \to 0$ and $\beta \to 1$ (and for constant film thickness) the results presented converge to those obtained by Grossman [12].

Initially, for small ξ, the interfacial film temperature and concentration are that predicted by the low penetration theory (equation (54a)) and $\theta_w = \phi_w = 0$. The behaviour in this region is the same for the adiabatic and isothermal wall cases. Increasing the concentration level affects significantly higher interfacial temperature due to higher absorption rates and thus lower interfacial concentration. A considerable deviation from the infinite dilution prediction (equation (54b)) is demonstrated for $X_{A_i} > 0.2$ ($\beta < 0.8$).

The location where the thermal boundary layer becomes fully developed ($\Delta_\theta = 1$ at $\xi = \xi_\theta$) marks the end of the first integration zone. This location is unaffected by the concentration level (see Fig. 6). As expected the concentration boundary layer develops considerably slower than the thermal boundary layer for the case studied with $Le \ll 1$, and is only partially developed at $\xi = \xi_\theta$. It reaches the fully developed thickness, $\Delta_\phi = 1$, at the end of the second integration zone where $\xi = \xi_\phi$. Accordingly, θ_w and ϕ_w start deviating from zero at $\xi = \xi_\theta$ and ξ_ϕ, respectively.

Figure 6(a) indicates that the concentration level hardly affects ξ_ϕ in the case of the isothermal wall. For the adiabatic wall case, however, the concentration boundary layer is shown to develop faster when the absorbate concentration level is increased (Fig. 6(b)). The resulting ξ_ϕ is always shorter than the corresponding value obtained under isothermal wall conditions.

Moving downstream, the trends observed for the variation of the film concentrations and temperature differs in the isothermal and adiabatic wall cases. In

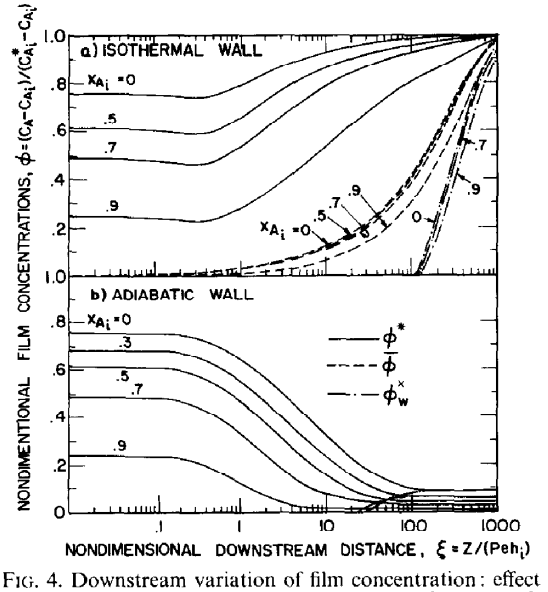

FIG. 4. Downstream variation of film concentration: effect of inlet absorbate concentration level, $Le = 10^{-3}$, $\Lambda = 10^{-2}$.

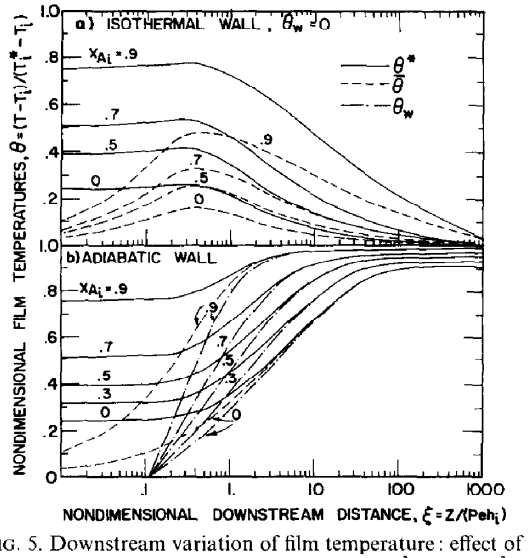

FIG. 5. Downstream variation of film temperature: effect of inlet absorbate concentration level, $Le = 10^{-3}$, $\Lambda = 10^{-2}$.

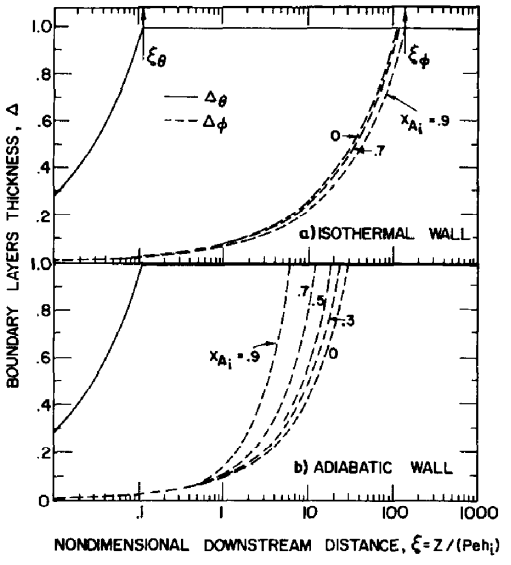

FIG. 6. Effect of inlet concentration level on the development of boundary layers.

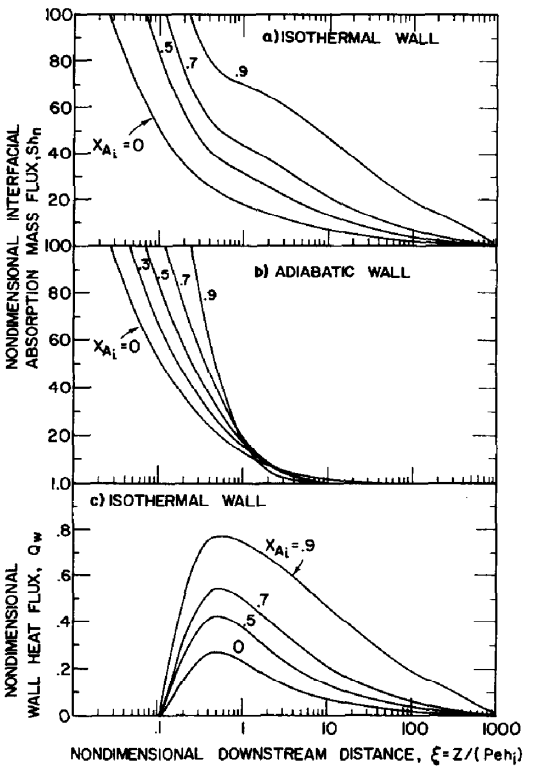

FIG. 7. Effect of inlet concentration level on the local non-dimensional absorption flux and wall heat flux.

the former case (Figs. 4(a) and 5(a)), the interfacial and bulk temperature first increase slightly, following the trend of zone 1, due to the heat released into the film. Then, for a sufficiently long transfer surface, the film temperature approaches the wall temperature and θ^*, $\bar{\theta}$ decrease, approaching zero as all the heat is removed through the wall. The interfacial absorbate concentrations follow trends opposite to that of the interfacial temperature ($\phi^* = 1-\theta^*$), with the wall, bulk and interfacial concentrations approaching 1 for $\xi \to \infty$. Hence, the effect of the concentration level diminishes in the downstream direction.

In the adiabatic wall case (Figs. 4(b) and 5(b)), the heat of absorption is not removed from the film. Consequently, the wall, bulk and interfacial temperatures increase monotonically towards a common asymptotic value. This final asymptotic value increases with increasing the concentration level, due to the enhanced absorption rates associated with higher absorbate concentration level (see also Fig. 7). Again, since $\phi^* = 1-\theta^*$, the interfacial concentration monotonically decreases downstream, towards its asymptotic value, which decreases with increasing the concentration level. Hence, for adiabatic wall conditions, the effect of the absorbate concentration level is sustained far downstream whereby (see Appendix B)

$$\theta_{\xi\to\infty} = \frac{\Lambda/\beta}{Le+\Lambda/\beta}; \quad \gamma \to 0$$

$$\phi_{\xi\to\infty} = \frac{Le}{Le+\Lambda/\beta}; \quad \gamma \to 0. \tag{75}$$

The corresponding values of the interfacial absorption (condensation) flux are presented in Fig. 7 in terms of Sh_n. It relates to the non-dimensional absorption flux defined in equation (19)

$$Sh_n = \frac{Le}{(-\gamma)Pe}\mathcal{N} = \frac{h_i}{D(C^*_{Ai}-C_{Ai})}\mathcal{N}_{AY}|_{Y=H}$$

$$= \frac{1}{\gamma\phi^*+\beta}\frac{\partial\phi}{\partial Y}\bigg|_{Y=H} \tag{76}$$

and is actually the Sherwood number which includes a nominal transfer coefficient, defined with reference to the nominal driving force, $Sh_n = K_n h_i/D$ ($K_n = N_{AY}/[C^*_{Ai}-C_{Ai}]$).

As is shown in Fig. 7(a) (isothermal wall), the absorption rates monotonically increase with increasing the absorbate concentration level. This enhancement reflects the augmentation of the mass transfer rate due to the inclusion of the convective term in equation (7). The enhanced absorption rates affect higher rates of heat removal through the isothermal wall (see Fig. 7(c)). Clearly, for a long transfer surface, the effect of concentration level on the transfer rates diminishes as the driving force for the absorption process ($\phi^*-\phi_w$) approaches zero.

In the adiabatic wall case (Fig. 7(b)), similar trends for the effect of the concentration level on the interfacial absorption rates are obtained for relatively short surfaces. Downstream, however, the augmentation of the transfer rates is damped due to the deterioration of the process driving force. Finally, for long transfer surfaces, this deterioration results in

lower local absorption rates for higher absorbate concentration levels.

The local transfer characteristics may be further studied through the downstream variation of local Sherwood and Nusselt numbers (based on the local transfer coefficient defined with respect to the local process driving force). The non-dimensional coefficient of local mass transfer from the interface to the bulk is given by

$$Sh = \frac{Kh_i}{D} = \frac{1}{H(\gamma\phi^* + \beta)(\phi^* - \bar{\phi})} \left.\frac{\partial\phi}{\partial\eta}\right|_{\eta=1}; \quad K = \frac{N_{AY}|_{Y=H}}{C_A^* - \bar{C}_A}. \tag{77}$$

The non-dimensional coefficient of local heat transfer from the interface to the bulk (due to the non-isothermal absorption) reads

$$Nu = \frac{h_T^* h_i}{k} = \frac{1}{H(\theta^* - \bar{\theta})} \left.\frac{\partial\theta}{\partial\eta}\right|_{\eta=1}; \quad h_T^* = \frac{\lambda_c N_{AY}|_{Y=H}}{(T^* - \bar{T})} \tag{78}$$

and the non-dimensional heat transfer coefficient from the bulk to the wall is given by

$$Nu_w = \frac{h_{T_w} h_i}{k} = \frac{1}{H(\bar{\theta} - \theta_w)} \left.\frac{\partial\theta}{\partial\eta}\right|_{\eta=0}; \quad h_{T_w} = \frac{q_w}{(\bar{T} - T_w)}. \tag{79}$$

Figure 8 describes the above local Sherwood and Nusselt numbers as a function of the downstream distance for the isothermal and adiabatic wall conditions (corresponding to Figs. 4–7). As expected, Sh is very large for small ξ where $\Delta_\phi \ll 1$ and decreases towards an asymptotic value reached at $\xi > \xi_\theta$ where $\Delta_\theta \equiv 1$. Evidently, the mass transfer coefficient increases with increasing the absorbate concentration level. Near the entry (zone 1), the behaviour is identical to the adiabatic and isothermal wall cases and the augmentation due to finite absorbate dilution is as in equation (71), $\Omega = 1/\beta$ (independent of Λ and Le). As the thermal boundary layer reaches the wall (zone 2, $\xi > \xi_\theta$) a discrepancy is noticed between the isothermal and adiabatic wall Sh, the former being larger and is more sensitive to the absorbate concentration level. Far downstream, an asymptotic value is reached, which is again identical for the adiabatic and isothermal wall conditions. Based on the analytic expression for $\bar{\theta}$, θ^*, θ_w derived in Appendix B, the asymptotic value which evolves from equation (77) is $40/11\beta$. Hence, the asymptotic augmentation of the mass transfer coefficient due to finite dilution (Sh_∞/Sh_∞^0) is again proportional to $1/\beta$. For infinite dilution ($\beta = 1$), $Sh_\infty = Sh_\infty^0 = 3.64$, which is about 5% larger than the exact value obtained by Grossman [13] for the case of infinite absorbate dilution. The overprediction of the transfer rates by the integral method is, however, higher upstream, in the low penetration region [12, 13]. Therefore, some overestimation of the concentration level effect in this region is expected [18, 19].

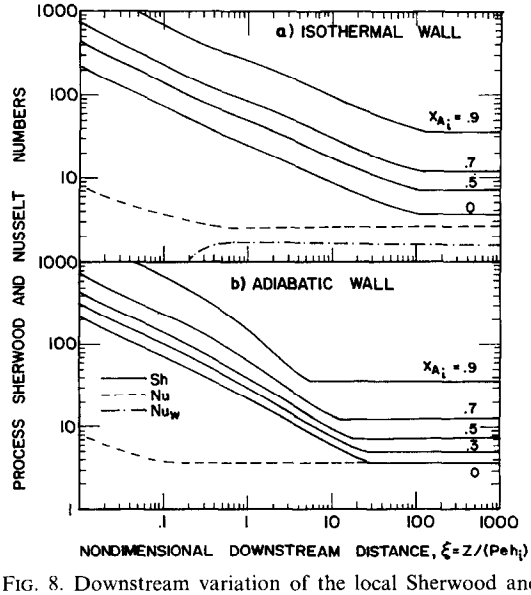

FIG. 8. Downstream variation of the local Sherwood and Nusselt numbers effect of the inlet concentration level.

The downstream variation of the interfacial and wall Nusselt numbers is considerably less pronounced. In the first zone, where $\Delta_\theta < 1$, the interfacial heat transfer coefficient decreases towards the asymptotic value, reached at $\xi > \xi_\theta$. Note that, for $\xi < \xi_\theta$, Nu is identical in the adiabatic and isothermal wall cases, while for $\xi > \xi_\theta$ the former is the larger. The asymptotic value (obtained by substitution of the analytic expressions derived for θ_w, θ^*, $\bar{\theta}$ in Appendix B into equation (78)) yields $Nu(\xi \to \infty) = 40/11$ for the adiabatic wall and $Nu(\xi \to \infty) = 8/3$ for isothermal wall conditions.

The wall heat transfer coefficient, Nu_w, is zero at the first integration zone, as the effects of condensation at the interface have not yet reached the wall. Beyond $\xi = \xi_\theta$, for the isothermal wall, Nu_w increases towards the asymptotic value $Nu_w(\xi \to \infty) = 1.6$. Obviously, $Nu_w \equiv 0$ for the adiabatic wall case. Note that both Nu and Nu_w are independent of the absorbate concentration level. Hence, the downstream decay of the heat transfer rates are determined by the deterioration of the temperature driving force (as discussed with reference to Fig. 5). Also, it is of interest to note that the asymptotic values of Sh, Nu, Nu_w are all independent of the other film parameters such as Le and Λ.

The discussion so far relates to the case of non-isothermal absorption under a low nominal process driving force, $\gamma \to 0$. For a finite driving force ($\gamma < 0$) the film flow rate increases downstream and its local thickness is to be evaluated through the integration of equation (46). Also, as it has been discussed with reference to Fig. 3, increasing the process driving force

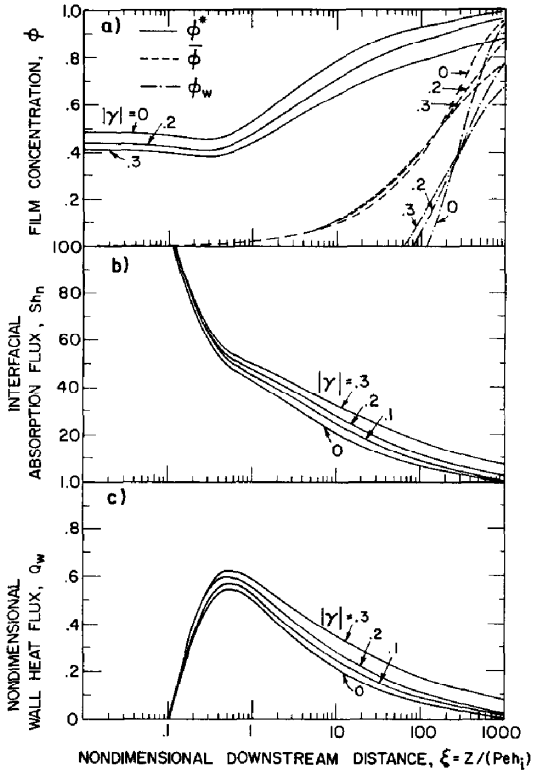

FIG. 9. Effect of the process driving force on the downstream film concentration, absorption rate and heat flux at the wall (isothermal wall).

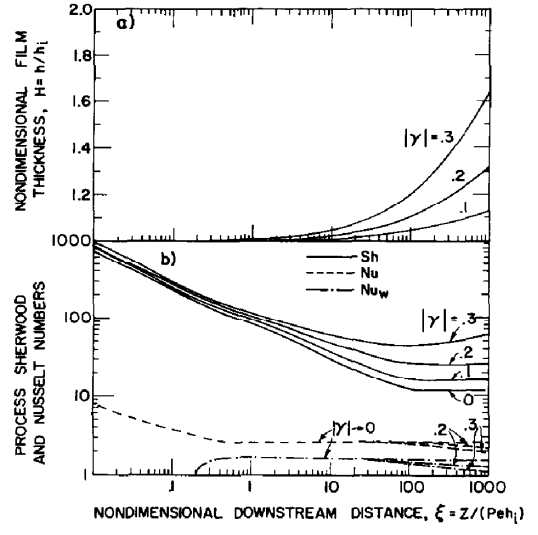

FIG. 10. Downstream variation of the local film thickness and local Sherwood and Nusselt numbers effect of process driving force (isothermal wall).

while maintaining Λ, Le and β constant affects higher interfacial temperature and thus lower interfacial absorbate concentrations.

The impact of increasing the driving force on the film transport characteristics is demonstrated through Figs. 9 and 10. The results are obtained for an isothermal wall with an inlet absorbate concentration of $X_{Ai} = 0.7$. The nominal driving force may be increased up to $\gamma = X_{Ai} - X^*_{Ai} = -0.3$, in which case the film interface (under an isothermal situation) consists of pure absorbate (pure water in the case of hygroscopic condensation on brine). Although the local driving force $\phi^* - \phi_w$ first decreases with $|\gamma|$ (small ξ in Fig. 9(a)), it recovers downstream, and the non-dimensional absorption flux (defined in equation (75)) as well as the heat removed through the wall increase with increasing the driving force (Figs. 9(b) and (c)). Consequently, the downstream film thickness becomes thicker, deviating from $H = 1$ (Fig. 10(a)). Clearly, a significant change in the film flow rate may be accompanied by a change in the film physical properties which is then to be accounted for.

The corresponding Sherwood and Nusselt numbers are shown in Fig. 10(b). It is noted that the interfacial and wall Nusselt numbers for $\xi \to \infty$ are here no longer constant. The decay of the asymptotic values with increasing the process driving force results from the downstream increase of the film thickness. On the other hand, the Sherwood number increases with increasing the driving force as expected, since the downstream absorbate concentration level increases towards X^*_{Ai}. However, comparison with the asymptotic values obtained for $\gamma \to 0$ (Fig. 8) reveals that the increase of Sh with $|\gamma|$ is damped due to the resulting thicker film and thus, it does not reach the asymptotic Sh obtained for $\beta = 1 - X^*_{Ai}$ with $\gamma \to 0$.

Similar trends (not shown here) have been obtained with an adiabatic wall condition, although it seems that for an adiabatic wall the effect of the process driving force is less pronounced and the results obtained with $\gamma \to 0$ are valid for a wider range of $\gamma \neq 0$. It is to be noted however, that a change of γ (for a given absorbing solution) affects a corresponding change of Λ, which is then to be accounted for. The exclusion of this change of Λ (Figs. 9 and 10) is aimed at isolating the influence of $\gamma \neq 0$ in comparison with the results obtained for $\gamma = 0$ (Figs. 4–8).

7. CONCLUDING REMARKS

A model is presented for the analysis of the combined heat and mass transfer involved in non-isothermal absorption of vapour into falling liquid film, as in hygroscopic film condensation. In distinction to absorption of sparingly soluble gases, characterized by infinite dilution of the absorbate, in vapour absorption the concentration levels of absorbate and absorbent are comparable.

The integral approach has been employed for solving simultaneously the continuity, diffusion and energy equations for the cases of an isothermal and adiabatic wall. Some analytic expressions are derived for limiting cases, such as low penetration, low process driving force and isothermal absorption.

The effect of the absorbate concentration level and process driving force on the film transfer characteristics has been studied. It has been shown that in

physical systems, where the absorbate concentration level is finite and is comparable to that of the absorbent component, the convective term in the lateral direction is to be accounted for. The inclusion of the convective term is of importance, as it results in enhanced transfer rates. Therefore, the use of empirical correlations, or models, obtained for infinite absorbate dilution, may yield conservative transfer rates in the design of hygroscopic condensation or evaporation systems [1–4].

REFERENCES

1. N. Brauner, D. Moalem Maron and S. Sideman, Heat and mass transfer in direct contact hygroscopic condensation, *Proc. 8th Int. Heat Transfer Conf.*, San Francisco, Vol. 4, pp. 1647–1652 (1986).
2. N. Brauner, D. Moalem Maron and S. Sideman, Heat and mass transfer in direct contact hygroscopic condensation, *Wärme- und Stoffübertr.* **21,** 233–245 (1987).
3. N. Brauner, D. Moalem Maron, Z. Harel and S. Sideman, Experimental studies of a hygroscopic condenser–evaporator heat exchanger based on concentration differences of vertically falling films, *Exp. Thermal Fluid Sci.* **2,** 392–409 (1989).
4. N. Brauner, D. Moalem Maron, Z. Harel and S. Sideman, Power recovery of concentration based energy sources by direct contact hygroscopic condensation on brine films. In *Energy Storage Systems: Fundamentals and Applications* (Edited by B. Kilkis and S. Kakac), Nato ASI Series E, Vol. 167, pp. 703–720. Kluwer, Dordrecht, The Netherlands (1989).
5. A. Bakopoulos, Liquid-side controlled mass transfer in wetted-wall tubes, *Germ. Chem. Engng* **3,** 241–252 (1980).
6. A. K. Bin, Mass transfer into turbulent liquid film, *Int. J. Heat Mass Transfer* **26,** 981–991 (1983).
7. S. M. Yih and K. Y. Chen, Gas absorption into wavy and turbulent falling liquid films in a wetted wall column, *Chem. Engng Commun.* **17,** 123–136 (1982).
8. G. Grossman, Heat and mass transfer in film absorption. In *Handbook of Heat and Mass Transfer* (Edited by N. P. Chezemisinoff), pp. 211–258. Gulf, Houston (1986).
9. S. M. Yih and R. C. Seagrave, Mass transfer in laminar falling liquid films with accompanying heat transfer and interfacial shear, *Int. J. Heat Mass Transfer* **23,** 749–758 (1980).
10. N. I. Grigor'eva and V. E. Nakoryakov, Exact solution of combined heat and mass transfer problem during film absorption, *Inzh.-fiz. Zh.* **33,** 983–989 (1977).
11. V. E. Nakoryakov and N. I. Grigor'eva, Calculation of heat and mass transfer in non-isothermal absorption in the entrance region of a falling film, *Teor. Osn. Khim. Tekhnol.* **14,** 483–488 (1980).
12. G. Grossman, Simultaneous heat and mass transfer in absorption desorption of gases in laminar liquid films, *Proc. A.I.Ch.E. Winter Annual Meeting*, Orlando, Florida (1982).
13. G. Grossman, Simultaneous heat and mass transfer in film absorption under laminar flow, *Int. J. Heat Mass Transfer* **26,** 357–371 (1983).
14. G. Grossman and M. T. Heath, Simultaneous heat and mass transfer in absorption of gases in turbulent liquid films, *Int. J. Heat Mass Transfer* **27,** 2365–2376 (1984).
15. A. Faghri and R. Seban, Heat and mass transfer to a turbulent liquid film, *Int. J. Heat Mass Transfer* **31,** 891–894 (1988).
16. A. Faghri and R. Seban, Heat and mass transfer to a turbulent falling film—II, *Int. J. Heat Mass Transfer* **32,** 1796–1798 (1989).
17. H. Le Goff, A. Ramadane, M. Barkaoui, Y. Chen and P. Le Goff, Modelling the coupled heat and mass transfer in falling film application to absorbers and desorbers in absorption heat pumps, *Proc. 8th Int. Heat Transfer Conf.*, San Francisco, Vol. 4, pp. 1971–1976 (1986).
18. N. Brauner, D. Moalem Maron and H. Meyrson, The effect of absorbate concentration level in hygroscopic condensation, *Commun. Heat Mass Transfer* **15**(3), 269–279 (1988).
19. N. Brauner, D. Moalem Maron and H. Meyerson, Coupled heat condensation and mass absorption with comparable concentrations of absorbate and absorbent, *Int. J. Heat Mass Transfer* **32,** 1897–1906 (1989).

APPENDIX A. MODEL DIFFERENTIAL EQUATIONS

Zone 1: $\Delta_\phi, \Delta_\theta \leqslant 1, \xi \leqslant \xi_\phi, \xi_\theta$

The prevailing equations are equations (46), (47a) and (48a). Equations (23) and (17) are used to eliminate Δ_θ, θ^* whereby

$$\theta^* = 1 - \phi^* \tag{A1}$$

$$\Delta_\theta = \frac{(1-\phi^*)(\gamma\phi^* + \beta)\Delta_\phi}{\Lambda\phi^*}. \tag{A2}$$

The derivation yields the following three simultaneous first-order differential equations for H, Δ_ϕ, ϕ^*:

$$\frac{dH}{d\xi} = -\frac{2}{3}\frac{\gamma\, Le}{H^3}\frac{\phi^*}{(\gamma\phi^* + \beta)\Delta_\phi}; \quad H(\xi = 0) = 1 \tag{A3}$$

$$\frac{d\Delta_\phi}{d\xi} = \frac{H^3\varepsilon_2\varepsilon_5 - \varepsilon_4}{H^3[\varepsilon_2\varepsilon_6 - \varepsilon_3]}; \quad \Delta_\phi(\xi = 0) = 0 \tag{A4}$$

$$\frac{d\phi^*}{d\xi} = \varepsilon_5 - \varepsilon_6\frac{H^3\varepsilon_2\varepsilon_5 - \varepsilon_4}{H^3[\varepsilon_2\varepsilon_6 - \varepsilon_3]};$$

$$\phi^*(\xi = 0) \text{ obtained by equation (53)} \tag{A5}$$

with

$$\varepsilon_1 = -\frac{1}{10}\left[\frac{(1-\phi^*)(\gamma\phi^* + \beta)\Delta_\phi}{\Lambda\phi^*}\right]^2$$

$$\varepsilon_2 = -\frac{\Delta_\phi}{2\Lambda}\frac{(1-\phi^*)}{\phi^{*2}}(2\gamma\phi^{*2} + \beta\phi^* + \beta)\varepsilon_1 + \frac{1}{10}\left[\frac{\Delta_\phi(1-\phi^*)}{\Lambda}\right]^3\frac{(\gamma\phi^* + \beta)^2(\gamma\phi^{*2} + \beta)}{\phi^{*4}}$$

$$\varepsilon_3 = \frac{(1-\phi^*)^2(\gamma\phi^* + \beta)}{2\Lambda\phi^*}\varepsilon_1 - \frac{\Delta_\phi^2(1-\phi^*)^4}{10}\left[\frac{(\gamma\phi^* + \beta)}{\Lambda\phi^*}\right]^3$$

$$\varepsilon_4 = \frac{2\Lambda}{H}\frac{\phi^*}{(\gamma\phi^* + \beta)\Delta_\phi}\left\{1 + Ja\,\theta^*\left[1 + \frac{\Delta_\theta}{2}(1 - \Delta_\phi^2/10)\right]\right\}$$

$$\varepsilon_5 = \frac{4Le\,\beta}{H^4}\frac{\phi^*}{(\gamma\phi^* + \beta)\Delta_\phi^2(1 - \Delta_\phi^2/10)}\left[1 + \frac{\gamma\phi^*\Delta_\phi}{2\beta}(1 - \Delta_\phi^2/10)\right]$$

$$\varepsilon_6 = \phi^*\frac{(1 - 3/10\Delta_\phi^2)}{(1 - 1/10\Delta_\phi^2)\Delta_\phi}. \tag{A6}$$

Evidently, the equations apply for both the adiabatic and constant wall temperature cases, since in zone 1 θ_w, ϕ_w, $Q_w \equiv 0$. The value of ξ where either Δ_ϕ or Δ_θ becomes equal to unity marks the end of zone 1.

Zone 2a: $\Delta_\theta \equiv 1, \Delta_\phi \leqslant 1, \xi_\phi \leqslant \xi \leqslant \xi_\phi$

For sufficiently low Le, the thermal boundary layer becomes fully developed first. In this region (where $\Delta_\theta \equiv 1$ and $\Delta_\phi \leqslant 1$) a distinction must be made between the adiabatic and constant temperature wall cases.

Constant temperature wall. The equations in effect are equations (46), (47a) and (48b). Equations (23) and (17) are used to obtain $\theta^* = 1 - \phi^*$ and

$$Q_w = 2\left[1-\phi^*-\frac{\Lambda\phi^*}{(\gamma\phi^*+\beta)\Delta_\phi}\right]. \tag{A7}$$

Substituting Q_w and θ^* yields the following three differential equations for H, Δ_ϕ, ϕ^*:

$$\frac{dH}{d\xi} = -\frac{2}{3}\frac{\gamma Le}{H^3}\frac{\phi^*}{(\gamma\phi^*+\beta)\Lambda_\phi} \tag{A8}$$

$$\frac{d\Delta_\phi}{d\xi} = \varepsilon_4 - \frac{\varepsilon_5\varepsilon_3}{H^3\varepsilon_1} \tag{A9}$$

$$\frac{d\phi^*}{d\xi} = \frac{\varepsilon_3}{H^3\varepsilon_1} \tag{A10}$$

$$\varepsilon_1 = 16+\frac{7\Lambda\beta}{(\gamma\phi^*+\beta)^2\Delta_\phi}+\frac{7\Lambda(1-\Delta_\phi^2/10)}{\Delta_\phi(1-3/10\Delta_\phi^2)(\gamma\phi^*+\beta)}$$

$$\varepsilon_2 = 1+\frac{\gamma\phi^*}{2\beta}\Delta_\phi(1-\Delta_\phi^2/10)$$

$$\varepsilon_3 = -\frac{40\Lambda\, Ja}{H}\frac{\phi^*}{(\gamma\phi^*+\beta)\Delta_\phi}\left[\frac{1}{5}(1-\phi^*)+\frac{7\Lambda\phi^*}{(\gamma\phi^*+\beta)\Delta_\phi}\right]+\frac{40}{H}\left[1-\phi^*-\frac{2\Lambda\phi^*}{(\gamma\phi^*+\beta)\Delta_\phi}\right]+\frac{28\Lambda\, Le\,\beta\phi^*}{H\Delta_\phi^3(\gamma\phi^*+\beta)^2(1-3/10\Delta_\phi^2)}\varepsilon_2$$

$$\varepsilon_4 = \frac{4Le\,\beta}{H^4}\frac{\varepsilon_2}{(\gamma\phi^*+\beta)\Delta_\phi(1-3/10\Delta_\phi^2)}$$

$$\varepsilon_5 = \frac{\Delta_\phi(1-\Delta_\phi^2/10)}{\phi^*(1-3/10\Delta_\phi^2)}. \tag{A11}$$

Adiabatic wall. The equations in effect are equations (46), (47a) and (48c). Utilizing equations (23) and (17) yields $\theta^* = 1-\phi^*$ and

$$\theta_w = 1-\phi^*-\frac{\Lambda\phi^*}{\Delta_\phi(\gamma\phi^*+\beta)}. \tag{A12}$$

The differential equations integrated to yield H, Δ_ϕ, ϕ^* in this case read

$$\frac{dH}{d\xi} = -\frac{2}{3}\frac{\gamma Le}{H^3}\frac{\phi^*}{(\gamma\phi^*+\beta)} \tag{A13}$$

$$\frac{d\Delta_\phi}{d\xi} = \varepsilon_4 - \frac{\varepsilon_5\varepsilon_3}{H^3\varepsilon_1} \tag{A14}$$

$$\frac{d\phi^*}{d\xi} = \frac{\varepsilon_3}{H^3\varepsilon_1} \tag{A15}$$

where

$$\varepsilon_1 = 1+\frac{11}{20}\frac{\Lambda}{\Delta_\phi(\gamma\phi^*+\beta)}\left[\frac{\beta}{\gamma\phi^*+\beta}+\frac{(1-\Delta_\phi^2/10)}{(1-3/10\Delta_\phi^2)}\right]$$

$$\varepsilon_2 = 1+\frac{\gamma\phi^*}{2\beta}\Delta_\phi(1-\Delta_\phi^2/10)$$

$$\varepsilon_3 = -\frac{11}{10}\frac{\Lambda^2\, Ja}{H}\left[\frac{\phi^*}{(\gamma\phi^*+\beta)\Delta_\phi}\right]^2-\frac{2\Lambda\phi^*}{H(\gamma\phi^*+\beta)\Delta_\phi}+\frac{11}{5}\frac{Le\,\beta\Lambda}{H}\frac{\phi^*\varepsilon_2}{(\gamma\phi^*+\beta)^2\Delta_\phi^3(1-3/10\Delta_\phi^2)}$$

$$\varepsilon_4 = \frac{4Le\,\beta}{H^4}\frac{\varepsilon_2}{(\gamma\phi^*+\beta)\Delta_\phi(1-3/10\Delta_\phi^2)}$$

$$\varepsilon_5 = \frac{\Delta_\phi(1-\Delta_\phi^2/10)}{\phi^*(1-3/10\Delta_\phi^2)}. \tag{A16}$$

The boundary conditions for both the adiabatic and constant wall temperature equations are defined by the values of (H, Δ_ϕ, ϕ^*) obtained through the integration of equations (A3)-(A5), at the end of the first zone (at $\xi = \xi_\theta$). The value of ξ where Δ_ϕ becomes equal to unity marks the end of zone 2a.

Zone 2b: $\Delta_\phi \equiv 1$, $\Delta_\theta \leqslant 1$

For relatively high Le and/or high absorbate concentration level, the concentration boundary layer develops faster than the thermal boundary layer and thus $\xi_\phi < \xi_\theta$. The equations in effect in this zone are equations (46), (47b) and (48a), and these apply for both the constant temperature and adiabatic wall conditions.

Equations (23) and (17) are utilized to express ϕ^*, ϕ_w in terms of (H, Δ_θ, ϕ^*) whereby

$$\theta^* = 1-\phi^*; \quad \phi_w = \phi^*-\frac{(1-\phi^*)(\gamma\phi^*+\beta)}{\Lambda\Delta_\theta}. \tag{A17}$$

The differential equations integrated to obtain H, Δ_θ, ϕ^* read

$$\frac{dH}{d\xi} = \frac{2}{3}\frac{Ja}{H^3}\frac{(1-\phi^*)}{\Delta_\theta} \tag{A18}$$

$$\frac{d\Delta_\theta}{d\xi} = \frac{1}{\varepsilon_4}\left[\varepsilon_2+\frac{\varepsilon_5\varepsilon_3}{H^3\varepsilon_1}\right] \tag{A19}$$

$$\frac{d\phi^*}{d\xi} = \frac{\varepsilon_3}{H^3\varepsilon_1} \tag{A20}$$

where

$$\varepsilon_1 = 1+\frac{11}{20\Lambda\Delta_\theta}\left[(2\gamma\phi^*+\beta-\gamma)+\frac{(\gamma\phi^*\beta)(1-\Delta_\theta^2/10)}{(1-3/10\Delta_\theta^2)}\right]$$

$$\varepsilon_2 = \frac{4Ja}{H}\frac{(1-\phi^*)^2}{\Delta_\theta}\left[1-\frac{1}{2}\Delta_\theta(1-\Delta_\theta^2/10)\right]+\frac{4(1-\phi^*)}{H\Delta_\theta}$$

$$\varepsilon_3 = \frac{2Le\,\beta}{H\Lambda}\frac{(1-\phi^*)}{\Delta_\theta}\left\{1+\frac{\gamma}{\beta}\left[\phi^*+\frac{11}{20\Lambda}\frac{(1-\phi^*)(\gamma\phi^*+\beta)}{\Delta_\theta}\right]\right\}-\frac{11}{20}\frac{(1-\phi^*)(\gamma\phi^*+\beta)}{\Lambda\Delta_\theta^2}\varepsilon_2$$

$$\varepsilon_4 = H^3(1-\phi^*)(1-3/10\Delta_\theta^2)$$

$$\varepsilon_5 = H^3\Delta_\theta(1-\Delta_\theta^2/10). \tag{A21}$$

The boundary conditions at $\xi = \xi_\phi$ are defined by the values of H, Δ_θ, ϕ^* obtained by carrying out the integration of the differential equations through zone 1 to the point where $\Delta_\phi = 1$. The values of ξ where Δ_θ becomes equal to unity marks the end of zone 2b.

Zone 3: Δ_θ, $\Delta_\phi \equiv 1$, $\xi > \xi_\theta$, ξ_ϕ

In this zone both boundary layers are fully developed. Again, a distinction is to be made between the constant wall temperature and adiabatic wall conditions.

Constant temperature wall. The equations prevailing are equations (46), (47b) and (48b). Equations (17) and (23) provide an expression for Q_w

$$Q_w = 2\left[1-\phi^*-\frac{\Lambda(\phi^*-\phi_w)}{(\gamma\phi^*+\beta)}\right] \tag{A22}$$

whereas (H, ϕ_w, ϕ^*) are obtained by integrating the following equations:

$$\frac{dH}{d\xi} = -\frac{2}{3}\frac{\gamma Le}{H^3}\frac{(\phi^*-\phi_w)}{(\gamma\phi^*+\beta)} \tag{A23}$$

$$\frac{d\phi_w}{d\xi} = \frac{\varepsilon_2}{H^3}-\frac{9}{11}\frac{\varepsilon_3}{H^3\varepsilon_1} \tag{A24}$$

$$\frac{d\phi^*}{d\xi} = \frac{\varepsilon_3}{H^3\varepsilon_1} \tag{A25}$$

where

$$\varepsilon_1 = 16+\frac{7\Lambda}{(\gamma\phi^*+\beta)}\left[\frac{\gamma\phi_w+\beta}{(\gamma\phi^*+\beta)}+\frac{9}{11}\right]$$

$$\varepsilon_2 = \frac{40}{11}\frac{Le\,\beta}{H}\frac{(\phi^*-\phi_w)}{(\gamma\phi^*+\beta)}\left[1+\frac{1}{20}\frac{\gamma}{\beta}(9\phi^*+11\phi_w)\right]$$

$$\varepsilon_3 = -\frac{2\Lambda\,Ja}{H}\frac{(\phi^*-\phi_w)}{(\gamma\phi^*+\beta)}\left[4(1-\phi^*)+\frac{7\Lambda(\phi^*-\phi_w)}{(\gamma\phi^*+\beta)}\right] + \frac{40}{H}\left[1-\phi^*-\frac{2\Lambda(\phi^*+\phi_w)}{(\gamma\phi^*+\beta)}\right]+\frac{7\Lambda}{(\gamma\phi^*+\beta)}\varepsilon_2. \quad \text{(A26)}$$

Adiabatic wall. The equations in effect are equations (46), (47b) and (48c). Equations (17) and (23) yield θ_w in terms of (ϕ^*, ϕ_w)

$$\theta_w = 1-\phi^*-\frac{\Lambda(\phi^*-\phi_w)}{(\gamma\phi^*+\beta)} \quad \text{(A27)}$$

whereas the resulting differential equations for (H, ϕ_w, ϕ^*) read

$$\frac{dH}{d\xi} = -\frac{2}{3}\frac{\gamma\,Le}{H^3}\frac{(\phi^*-\phi_w)}{(\gamma\phi^*+\beta)} \quad \text{(A28)}$$

$$\frac{d\phi_w}{d\xi} = \frac{20}{11}\frac{\varepsilon_2}{H^3}-\frac{9}{11}\frac{\varepsilon_3}{H^3\varepsilon_1} \quad \text{(A29)}$$

$$\frac{d\phi^*}{d\xi} = \frac{\varepsilon_3}{H^3\varepsilon_1} \quad \text{(A30)}$$

where

$$\varepsilon_1 = 1+\frac{11}{20}\frac{\Lambda}{(\gamma\phi^*+\beta)}\left[\frac{9}{11}+\beta+\gamma\phi_w\right]$$

$$\varepsilon_2 = \frac{2Le\,\beta}{H}\frac{(\phi^*-\phi_w)}{(\gamma\phi^*+\beta)}\left[1+\frac{1}{20}\frac{\gamma}{\beta}(9\phi^*+11\phi_w)\right]$$

$$\varepsilon_3 = -\frac{11}{10}\frac{\Lambda^2\,Ja}{H}\left[\frac{(\phi^*-\phi_w)}{(\gamma\phi^*+\beta)}\right]^2 - \frac{2\Lambda}{H}\left[\frac{(\phi^*-\phi_w)}{(\gamma\phi^*+\beta)}\right]+\frac{\varepsilon_2\Lambda}{(\gamma\phi^*+\beta)}. \quad \text{(A31)}$$

The boundary conditions used for integrating either equations (A23)–(A25) or equations (A28)–(A30) are the values obtained for H, ϕ_w and ϕ^* at the end of the second zone. The integration in the fully developed boundary layer region is carried on downstream until uniform concentration and temperature profiles are obtained across the film, as equilibrium is reached.

APPENDIX B. MODEL EQUATIONS FOR $\beta \neq 1$, $\gamma \to 0$, $Ja \ll 1$

In the limit of a low process driving force, $\gamma \to 0$, $\gamma\phi^*+\beta \to \beta$ and by equation (46) $H = 1$. Under these conditions, the model equations (equations (47) and (48)) are significantly simplified and some analytic solutions may be derived in terms of a combined parameter Λ/β (instead of both Λ and β in the general case).

Zone 1

$$\frac{d}{d\xi}\left[\frac{\phi^*}{2}\Delta_\phi\left(1-\frac{\Delta_\phi^2}{10}\right)\right] = \frac{2Le\,\phi^*}{\Delta_\phi} \quad \text{(B1)}$$

$$\frac{d}{d\xi}\left[\frac{\theta^*}{2}\Delta_\theta\left(1-\frac{\Delta_\theta^2}{10}\right)\right] = \frac{2\Lambda}{\beta}\frac{\phi^*}{\Delta_\phi} \quad \text{(B2)}$$

$$\theta^*+\phi^* = 1 \quad \text{(B3)}$$

$$\frac{\theta^*}{\Lambda_\theta} = \frac{\Lambda}{\beta}\frac{\phi^*}{\Delta_\phi}. \quad \text{(B4)}$$

For $Le < 1$, $\Delta_\phi < \Delta_\theta$, equations (B1)–(B4) are solved to yield

$$\Delta_\phi = \sqrt{(Le)}\Delta_\theta(1-\Delta_\theta^2/10)^{1/2} \quad \text{(B5)}$$

$$\theta^* = \frac{1}{1+\frac{\sqrt{(Le)}}{\Lambda/\beta}(1-\Delta_\theta^2/10)^{1/2}};$$

$$\phi^* = \frac{\frac{\sqrt{(Le)}}{\Lambda/\beta}(1-\Delta_\theta^2/10)^{1/2}}{1+\frac{\sqrt{(Le)}}{\Lambda/\beta}(1-\Delta_\theta^2/10)^{1/2}} \quad \text{(B6)}$$

$$\bar{\theta} = \frac{1}{2}\frac{\Delta_\theta(1-\Delta_\theta^2/10)}{1+\frac{\sqrt{(Le)}}{\Lambda/\beta}(1-\Delta_\theta^2/10)^{1/2}};$$

$$\bar{\phi} = \frac{1}{2}\frac{Le}{\Lambda/\beta}\frac{\Delta_\theta(1-\Delta_\theta^2/10)}{1+\frac{\sqrt{(Le)}}{\Lambda/\beta}(1-\Delta_\theta^2/10)^{1/2}} \quad \text{(B7)}$$

$$\xi = \frac{\Delta_\theta^2}{8}\left[1-\frac{\Delta_\theta^2}{10}\frac{1+1.5\Lambda/(Le\,\beta)}{1+\Lambda/(Le\,\beta)}\right];$$

$$\xi_\theta = \frac{9}{80}\left[\frac{1+17/18\Lambda/(Le\,\beta)}{1+\Lambda/(Le\,\beta)}\right]. \quad \text{(B8)}$$

Zone 2a

Isothermal wall.

$$\frac{d}{d\xi}\left[\frac{\phi^*}{2}\left(\Delta_\phi-\frac{\Delta_\phi^3}{10}\right)\right] = \frac{2Le\,\phi^*}{\Delta_\phi} \quad \text{(B9)}$$

$$\frac{d}{d\xi}\left[\frac{1}{40}(18\theta^*+7Q_w)\right] = \frac{2\Lambda\phi^*}{\beta\Delta_\phi}-Q_w \quad \text{(B10)}$$

$$\theta^*+\phi^* = 1 \quad \text{(B11)}$$

$$2\theta^*-Q_w = \frac{2\Lambda}{\beta}\frac{\phi^*}{\Delta_\phi}. \quad \text{(B12)}$$

No simple analytic expressions are obtained in this case and the integration is to be carried out numerically.

Adiabatic wall.

$$\frac{d}{d\xi}\left[\frac{\phi^*}{2}\left(\Delta_\phi-\frac{\Delta_\phi^3}{10}\right)\right] = 2Le(\theta^*-\theta_w) \quad \text{(B13)}$$

$$\frac{d}{d\xi}\left[\frac{1}{20}(9\theta^*+11\theta_w)\right] = \frac{2\Lambda}{\beta}\frac{\phi^*}{\Delta_\phi} \quad \text{(B14)}$$

$$\theta^*+\phi^* = 1 \quad \text{(B15)}$$

$$\theta^*-\theta_w = \frac{\Lambda}{\beta}\frac{\phi^*}{\Delta_\phi}. \quad \text{(B16)}$$

Equations (B13)–(B16) yield

$$\theta^* = \frac{\frac{\Lambda/\beta}{2\Delta_\phi}\left[\frac{11}{10}+\frac{\Delta_\phi^2}{Le}(1-\Delta_\phi^2/10)\right]}{1+\frac{\Lambda/\beta}{2\Delta_\phi}\left[\frac{11}{10}+\frac{\Delta_\phi^2}{Le}(1-\Delta_\phi^2/10)\right]}; \quad \phi^* = 1-\theta^* \quad \text{(B17)}$$

$$\theta_w = \frac{\frac{\Lambda/\beta}{2\Delta_\phi}\left[-\frac{9}{10}+\frac{\Delta_\phi^2}{Le}(1-\Delta_\phi^2/10)\right]}{1+\frac{\Lambda/\beta}{2\Delta_\phi}\left[\frac{11}{10}+\frac{\Delta_\phi^2}{Le}(1-\Delta_\phi^2/10)\right]} \quad \text{(B18)}$$

$$\bar{\theta} = \frac{\Lambda/\beta}{2Le}\frac{\Delta_\phi(1-\Delta_\phi^2/10)}{1+\frac{\Lambda/\beta}{2\Delta_\phi}\left[\frac{11}{10}+\frac{\Delta_\phi^2}{Le}(1-\Delta_\phi^2/10)\right]}; \quad \bar{\phi} = \frac{\bar{\theta}\,Le}{\Lambda/\beta}. \quad \text{(B19)}$$

The variation of $\Delta_\phi(\xi)$ is obtained through a numerical inte-

gration of equation (B13) with $\Lambda_\phi = \sqrt{(9Le/10)}$ at $\xi = \xi_\theta$ (see equations (B5) and (B8) with $\Delta_\theta = 1$).

Zone 3

Isothermal wall.

$$\frac{\mathrm{d}}{\mathrm{d}\xi}\left[\frac{1}{20}(9\phi^* + 11\phi_w)\right] = 2(\phi^* - \phi_w) \tag{B20}$$

$$\frac{\mathrm{d}}{\mathrm{d}\xi}\left[\frac{1}{40}(18\theta^* + 7Q_w)\right] = \frac{2\Lambda}{\beta}(\phi^* - \phi_w) - Q_w \tag{B21}$$

$$\theta^* + \phi^* = 1 \tag{B22}$$

$$2\theta^* - Q_w = \frac{2\Lambda}{\beta}(\phi^* - \phi_w). \tag{B23}$$

Analytic integration carried out with the boundary condition $\phi_w = 0$, $\phi_2^* = \phi^*(\xi = \xi_\phi)$ (as obtained from the solution for zone 2) yields

$$\frac{(1-\phi^*) - 2\Lambda/\beta(\phi^* - \phi_w)}{(1-\phi_2^*) - 2\Lambda/\beta\phi_2^*} = \left[\frac{1-(9\phi^* + 11\phi_w)/20}{1-9\phi_2^*/20}\right]^{((11+40\Lambda/\beta)16Le)} = \left[\frac{1-\bar{\phi}}{1-\bar{\phi}_2}\right]^{((11+40\Lambda/\beta)16Le)} \tag{B24}$$

where $\bar{\phi}_2 = \bar{\phi}(\xi = \xi_\phi)$, and thus $(1-\bar{\phi})/(1-\bar{\phi}_2) < 1$. For $Le \ll 1$ the right-hand side of equation (B24) approaches zero, whereby

$$\phi^* = (1 + 2\Lambda/\beta\phi_w)/(1 + 2\Lambda/\beta)\ ; \quad \theta^* = 1 - \phi^* \tag{B25}$$

which yields

$$Q_w = 2\Lambda/\beta(1-\phi_w)/(1+2\Lambda/\beta) \tag{B26}$$

$$\bar{\theta} = \frac{5\Lambda/\beta(1-\phi_w)}{4(1+2\Lambda/\beta)}\ ; \quad \bar{\phi} = \frac{9 + 11\phi_w + 40(\Lambda/\beta)\phi_w}{20(1+2\Lambda/\beta)}. \tag{B27}$$

Integration of equation (B20) with ϕ^* by equation (B25) yields

$$\phi_w = 1 - \exp\left[-\frac{40Le}{(11+40\Lambda/\beta)}(\xi - \xi_\phi)\right]. \tag{B28}$$

Adiabatic wall.

$$\frac{\mathrm{d}}{\mathrm{d}\xi}\left[\frac{1}{20}(9\phi^* + 11\phi_w)\right] = 2Le(\phi^* - \phi_w) \tag{B29}$$

$$\frac{\mathrm{d}}{\mathrm{d}\xi}\left[\frac{1}{20}(9\theta^* + 11\theta_w)\right] = \frac{2\Lambda}{\beta}(\phi^* - \phi_w) \tag{B30}$$

$$\theta^* + \phi^* = 1 \tag{B31}$$

$$(\theta^* - \theta_w) = \frac{\Lambda}{\beta}(\phi^* - \phi_w). \tag{B32}$$

Equations (B29)–(B32) for $Le \ll 1$ yield

$$\phi^* = [1 - (11/20)(\Lambda/\beta\, Le)\phi_w]/[1 + (9/20)(\Lambda/\beta\, Le)]\,;$$

$$\theta^* = 1 - \phi^* \tag{B33}$$

$$\theta_w = \theta^* - \frac{\Lambda}{\beta}\frac{1-\phi_w - (\Lambda/\beta\, Le)\phi_w}{1 + (9/20)(\Lambda/\beta\, Le)} \tag{B34}$$

$$\bar{\theta} = \frac{\Lambda/\beta}{Le}\left[\frac{9/20 + (11/20)\phi_w + (11/20)(\Lambda/\beta)\phi_w}{1 + (9/20)(\Lambda/\beta\, Le)}\right];$$

$$\bar{\phi} = \frac{Le}{\Lambda/\beta}\bar{\theta} \tag{B35}$$

$$\phi_w = \frac{Le}{Le + \Lambda/\beta}\left\{1 - \exp\left[-\frac{40}{11}\frac{(Le + \Lambda/\beta)}{(1+\Lambda/\beta)}(\xi - \xi_\phi)\right]\right\}. \tag{B36}$$

ABSORPTION NON ISOTHERME DE VAPEUR DANS UN FILM TOMBANT

Résumé—L'étude concerne l'absorption de vapeur dans un film tombant pour lequel les concentrations d'absorbat et d'absorbant sont comparables. Les mécanismes combinés de transfert de chaleur et de masse sont analysés à travers une formulation intégrale des équations de continuité, de diffusion et d'énergie. On considère des conditions de paroi adiabatique et isotherme. Les nombres de Nusselt et de Sherwood sont exprimés en fonction des paramètres adimensionnels qui caractérisent le système. On montre que dans le cas de la dilution finie d'absorbat, le terme convectif latéral à la surface libre doit être pris en compte. Le transfert résultant dépend à la fois du niveau de concentration d'absorbat et de la force motrice et il est significativement augmenté par rapport à ce qui est obtenu dans l'hypothèse d'une dilution infinie d'absorbat.

DIE NICHTISOTHERME ABSORPTION VON DAMPF IN EINEM RIESELFILM

Zusammenfassung—Die vorliegende Untersuchung beschäftigt sich mit der Absorption von Dampf in einem Rieselfilm, und zwar für den Fall, daß sich die Konzentrationen in Dampf und Flüssigkeit wenig unterscheiden. Zur Analyse der gekoppelten Vorgänge des Wärme- und Stofftransports wird eine Integralform der Kontinuitäts-, der Diffusions- und der Energiegleichung betrachtet. Die Wand wird als adiabat bzw. isotherm angenommen. Die Nusselt- und die Sherwood-Zahl werden abhängig von dimensionslosen Parametern ausgedrückt, welche das System beschreiben. Es zeigt sich, daß eine endliche Verdünnung des zu absorbierenden Stoffes durch einen entsprechenden quergerichteten Konvektionsterm an der freien Oberfläche berücksichtigt werden sollte. Es zeigt sich weiterhin, daß die resultierenden Wärme- und Stoffströme sowohl von der Konzentration im zu absorbierenden Stoff abhängen als auch von der treibenden Kraft; sie sind wesentlich größer im Vergleich zu denjenigen, welche sich bei Annahme einer unendlich kleinen Verdünnung ergeben.

НЕИЗОТЕРМИЧНОЕ ПОГЛОЩЕНИЕ ПАРА СТЕКАЮЩЕЙ ПЛЕНКОЙ

Аннотация—Исследуется поглощение пара стекающей пленкой при сопоставимых концентрациях абсорбата и абсорбента. Совместные процессы тепло- и массопереноса анализируются при помощи уравнений разрывности, диффузии и энергии в интегральной форме. Рассматриваются условия с адиабатической и изотермической стенками. Числа Нуссельта и Шервуда выражены через безразмерные параметры, характеризующие систему. Показано, что в случае конечного разбавления абсорбата следует учитывать слагаемое, описывающее поперечную конвекцию у свободной поверхности. Найдено, что результирующие скорости зависят как от концентрации абсорбата, так и от движущей силы и заметно превышают значения, полученные в предположении бесконечного разбавления абсорбата.